

# **Tuning the Electrochemical Properties of Transition Metal Oxide Anode based Material for Li-Ion Batteries**



By

Ammar Ud Din

(Registration No: 00000399848)

Department of Materials Engineering

School of Chemical and Materials Engineering

National University of Sciences & Technology (NUST)

Islamabad, Pakistan

(2024)

# **Tuning the Electrochemical Properties of Transition Metal Oxide Anode based Material for Li-Ion Batteries**



By

Ammar Ud Din

(Registration No: 00000399848)

A thesis submitted to the National University of Sciences and Technology, Islamabad,

in partial fulfillment of the requirements for the degree of

Master of Science in  
Nanoscience and Engineering

Supervisor: Dr. Amna Safdar

Co Supervisor: Dr. Mashkoor Ahmad

School of Chemical and Materials Engineering

National University of Sciences & Technology (NUST)

Islamabad, Pakistan

(2024)

# THESIS ACCEPTANCE CERTIFICATE



## THESIS ACCEPTANCE CERTIFICATE

Certified that final copy of MS Thesis entitled "Turning the Electrochemical Properties of Transition Metal Oxide Anode based Material for Li-Ion Batteries" written by Mr Ammar Ud Din (Registration No 00000399848), of School of Chemical & Materials Engineering (SCME) has been vetted by undersigned, found complete in all respects as per NUST Statues/Regulations, is free of plagiarism, errors, and mistakes and is accepted as partial fulfillment for award of MS degree. It is further certified that necessary amendments as pointed out by GEC members of the scholar have also been incorporated in the said Thesis.

Signature: \_\_\_\_\_

Name of Supervisor: Dr Amna Safdar

Date: 20/11/2024

Signature (HOD): \_\_\_\_\_

Date: 22-11-24

For Signature (Dean/Principal): \_\_\_\_\_

Date: 22/11/24

# TH - 1

Form TH-1

## National University of Sciences & Technology (NUST) MASTER'S THESIS WORK

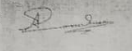
Formulation of Guidance and Examination Committee (GEC)

Name: Ammar Ud Din NUST Reg No: 00000399848  
Department: Department of Materials Engineering Specialization: Master of Science in Nanoscience and Engineering  
Credit Hour Completed: 24.0 CGPA: 3.75

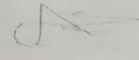
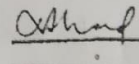
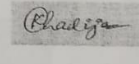
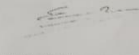
### Course Work Completed

S/No:	Code:	Title:	Core/Elective:	CH:	Grade:
1.	NSE-813	Essentials of Nanoscience and Engineering	Compulsory	3.0	B+
2.	MSE-854	Characterization Of Materials	Compulsory	3.0	A
3.	RM-898	Research Methodology	Additional	2.0	Q
4.	NSE-843	Nano Technology And Photovoltaics	Elective	3.0	B+
5.	MSE-856	Nano Material and Processing	Compulsory	3.0	A
6.	MSE-954	Advanced Characterization Techniques	Elective	3.0	A
7.	ESE-836	Li-ion and Next Generation Batteries	Elective	3.0	B
8.	NSE-842	Nano Materials For Energy Applications	Elective	3.0	A
9.	NSE-845	Nanolithography And Device Fabrication	Elective	3.0	A

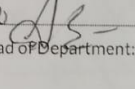
Date 28 - Mar - 2024

Student's Signature 

### Thesis Committee

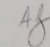
- Name: Amna Safdar (Supervisor) Signature   
Department: Department of Materials Engineering
- Name: Nasir Mahmood Ahmad (Internal) Signature   
Department: Department of Materials Engineering
- Name: Khadija Munawar (Internal) Signature   
Department: Department of Chemistry
- Name: Muhammad Syar (Internal) Signature   
Department: Department of Materials Engineering

Date: 28 - Mar - 2024

DR. Mashkoor Ahmed For  
Co-Supervisor Signature of Head of Department: 

### APPROVAL

Date: 28 - Mar - 2024

Signature of Dean/Principal: 

# TH - 4



National University of Sciences & Technology (NUST)

FORM TH-4

MASTER'S THESIS WORK

We hereby recommend that the dissertation prepared under our supervision by

Regn No & Name: 00000399848 Ammar Ud Din

Title: Turning the Electrochemical Properties of Transition Metal Oxide Anode based Material for Li-Ion Batteries.

Presented on: 07 Nov 2024 at: 1500 hrs in SCME Seminar Hall

Be accepted in partial fulfillment of the requirements for the award of Masters of Science degree in Nanoscience & Engineering.

### Guidance & Examination Committee Members

Name: Dr Nasir M. Ahmed

Signature: [Signature]

Name: Dr Muhammad Siyar

Signature: [Signature]

Name: Dr Khadija Munawar

Signature: [Signature]

Name: Dr Mashkoor Ahmad (Co-Supervisor)

Signature: [Signature]

Supervisor's Name: Dr Amna Safdar

Signature: [Signature]

Dated: 07/11/2024

[Signature]  
Head of Department

12-11-24  
Date

COUNTERSIGNED

Date \_\_\_\_\_

[Signature]  
Dean/Principal

## **AUTHOR'S DECLARATION**

I **Ammar Ud Din** hereby state that my MS thesis titled “**Tuning the Electrochemical Properties of Transition Metal Oxide Anode based Material for Li-Ion Batteries**” is my own work and has not been submitted previously by me for taking any degree from National University of Sciences and Technology, Islamabad or anywhere else in the country/ world.

At any time if my statement is found to be incorrect even after I graduate, the university has the right to withdraw my MS degree.

Name of Student: Ammar Ud Din

Date: 22 November 2024

## **PLAGIARISM UNDERTAKING**

I solemnly declare that research work presented in the thesis titled “Tuning the Electrochemical Properties of Transition Metal Oxide Anode Based Material for Energy Storage Applications” is solely my research work with no significant contribution from any other person. Small contribution/ help wherever taken has been duly acknowledged and that complete thesis has been written by me.

I understand the zero-tolerance policy of the HEC and National University of Sciences and Technology (NUST), Islamabad towards plagiarism. Therefore, I as an author of the above titled thesis declared that no portion of my thesis has been plagiarized and any material used as reference is properly referred/cited.

I undertake that if I am found guilty of any formal plagiarism in the above titled thesis even after award of MS degree, the University reserves the rights to withdraw/revoke my MS degree and that HEC and NUST, Islamabad has the right to publish my name on the HEC/University website on which names of students are placed who submitted plagiarized thesis.

Student Signature:

Name: Ammar Ud Din

## DEDICATION

*This work is **dedicated** to **Allah Almighty**, whose boundless blessings, mercy, and guidance have been my strength throughout this journey. To my **beloved parents**, whose unwavering love, support, and sacrifices have been the cornerstone of my success. Your belief in me has been my greatest motivation.*

*To my **brothers and sisters**, for their constant encouragement, love, and patience. Your support has been invaluable in this long academic journey. This achievement is as much yours as it is mine.*



## ACKNOWLEDGEMENTS

First and foremost, I would like to express my deepest gratitude to **Allah Almighty**, whose countless blessings have guided me throughout this journey. Without His mercy and guidance, this work would not have been possible.

A special note of appreciation goes to my **teachers and mentors**, who have been instrumental in my academic journey. I am especially grateful to **Dr. Amna Safdar, Dr. Mashkooor Ahmad** and **Dr. Amjad** for their invaluable guidance, encouragement, and support. I also like to thank my GEC member Dr Nasir Ahmad, Dr Khandija Monawar. Your insightful feedback and continuous encouragement have shaped the direction of my research, and I am forever grateful for the knowledge and wisdom you have imparted to me.

I would like to extend my heartfelt thanks to my **family**. To my parents, for their endless support, unconditional love, and encouragement throughout my academic career. Their patience and prayers have been the foundation of my strength, and their unwavering belief in me kept me going during the most challenging times.

To my **friends**, who have always been there to share my triumphs and provide solace in moments of frustration. Your constant support, humor, and encouragement have been a source of motivation for me. Thank you for understanding when I could not spend time with you and for always believing in my potential.

To all those who have played a role in this journey, whether mentioned or not, thank you for your presence in my life. This achievement is as much yours as it is mine.

**Ammar Ud Din**

## TABLE OF CONTENTS

<b>ACKNOWLEDGEMENTS</b>	<b>IX</b>
<b>TABLE OF CONTENTS</b>	<b>IX</b>
<b>LIST OF TABLES</b>	<b>XI</b>
<b>LIST OF FIGURES</b>	<b>XII</b>
<b>LIST OF SYMBOLS, ABBREVIATIONS AND ACRONYMS</b>	<b>XIV</b>
<b>ABSTRACT</b>	<b>XV</b>
<b>CHAPTER 1: INTRODUCTION</b>	<b>1</b>
<b>1.1 Motivation</b>	<b>1</b>
1.1.1 Batteries Verses Supercapacitor Verses Fuel Cell	2
<b>1.2 Lithium-ion Batteries Era</b>	<b>3</b>
<b>1.3 Basic of Lithium-ion Batteries</b>	<b>4</b>
<b>1.4 Why Lithium-ion Batteries</b>	<b>7</b>
<b>1.5 Cathode</b>	<b>11</b>
<b>1.6 Electrolyte</b>	<b>12</b>
<b>1.7 Separator</b>	<b>12</b>
<b>1.8 Anode</b>	<b>13</b>
1.7.1 Anode Material for Lithium-Ion Batteries	13
1.7.2 Insertion type	13
1.7.3 Alloy type	16
1.7.4 Conversion type	17
<b>CHAPTER 2: LITERATURE REVIEW</b>	<b>20</b>
<b>2.1 Iron Oxides</b>	<b>20</b>
<b>2.2 Nickel Oxides</b>	<b>23</b>
<b>2.3 Hollwo carbon spheres</b>	<b>26</b>
<b>2.4 Fe<sub>3</sub>O<sub>4</sub>/NiO composite</b>	<b>27</b>
<b>CHAPTER 3: EXPERIMENTATION</b>	<b>30</b>
<b>3.1 Synthesis of NiO</b>	<b>30</b>
<b>3.2 Synthesis of Fe<sub>3</sub>O<sub>4</sub></b>	<b>31</b>
<b>3.3 Synthesis of Hollow Carbon Spheres</b>	<b>32</b>
<b>3.6 Fabrication of Coin Cell</b>	<b>33</b>
3.6.1 Slurry Preparation	33
3.6.2 Coin Cell Assembly	35
<b>3.4 Synthesis of Fe<sub>3</sub>O<sub>4</sub>/NiO</b>	<b>36</b>
<b>3.5 Synthesis of Fe<sub>3</sub>O<sub>4</sub>/NiO@HCSs</b>	<b>36</b>

<b>CHAPTER 4: RESULTS AND DISCUSSION</b>	<b>38</b>
<b>4.1 X-Ray Diffraction (XRD)</b>	<b>38</b>
<b>4.2 Scanning Electron Microscopy (SEM)</b>	<b>39</b>
<b>4.3 Raman Spectroscopy</b>	<b>41</b>
<b>4.4 FTIR Spectroscopy</b>	<b>42</b>
<b>4.5 X-Photoelectron Spectroscopy (XPS)</b>	<b>43</b>
<b>4.6 Electrochemical Impedance Spectroscopy (EIS)</b>	<b>45</b>
<b>4.7 Cyclic Voltammetry (CV)</b>	<b>46</b>
<b>4.8 Galvanic Charge and Discharging (GCD)</b>	<b>48</b>
<b>CHAPTER 5: CONCLUSIONS</b>	<b>51</b>
<b>5.1 Conclusions</b>	<b>51</b>
<b>REFERENCES</b>	<b>52</b>

## LIST OF TABLES

	<b>Page No.</b>
<b>Table 1.1</b> Shows the basic difference of Primary and secondary batteries.....	5
<b>Table 2.1</b> Investigated the Fe <sub>3</sub> O <sub>4</sub> with Different Strategies and Composite with Carbon. ....	21
<b>Table 2.2</b> Investigated the NiO with Different Strategies and Composite Materials. ....	25

## LIST OF FIGURES

	Page No.
<b>Figure 1.1:</b> Ragone plot of different types of batteries technology with different specifications at cell level for the application of automobile .....	2
<b>Figure 1.2:</b> Ragon plot for Supercapacitor, Fuel cell and batteries against specific Energy density and power density with permission [9].....	3
<b>Figure 1.3:</b> Shows the first lithium-ion battery pattern By Yohsino, the cathode is LiCoO <sub>2</sub> against carbon Represent by 1 and 2. The number 3 is current colector, 4 shows the SUS nets, 5 external electrodes Terminal, 6 case, 7 separator, 8 electrolyte 9 .....	4
<b>Figure 1.4:</b> Schematic illustrate assembly and working mechanism of Lithium-ion batteries. ....	6
<b>Figure 1.5:</b> Trend shows the increasing demands of lithium-ion batteries compared to other types of batteries with time12 .....	7
<b>Figure 1.6:</b> Schematic shows the investigated material used as anode and cathode for lithium-ion batteries. ....	10
<b>Figure 1.7:</b> Shows widely investigated cathode material used in commercialize lithium-ion batteries. ....	11
<b>Figure 1.8:</b> The Ragon shows the invstefated anode material for lithium ion battereis against the capacity and potential. ....	14
<b>Figure 1.9:</b> Schematic illustrate the different type structural carbonesious materia used for lithium ion batteries [20] .....	15
<b>Figure 1.10:</b> Schematic shows the structure and reaction mechanism of insertion, alloy and conversion types of materials. ....	18
<b>Figure 2.1</b> Crystal structure of Fe <sub>3</sub> O <sub>4</sub> genrated from the data base of material project. 20	20
<b>Figure 2.2:</b> Plote shows the crystal structure Nickel Oxide which is take out from the material project data. ....	24
<b>Figure 2.3:</b> Schematic illustrate the types of hollow carbon spheres with different types of morphologies used for the application of Energy storage devices.....	26
<b>Figure 3.1:</b> Image illustrate during the grinding of composite material.....	30
<b>Figure 3.2:</b> Schematic shows the step by step synthessi of nickel oxide nanoparticles through co-precipetation method. ....	31
<b>Figure 3.3:</b> Schematic shows the preperation step of iron ocides nanoparticles. ....	32
<b>Figure 3.4:</b> Schematic show the step by step procedur and effect of ration of ethanol and water effects on hollow carbon spheres. ....	33
<b>Figure 3.5:</b> Image shows the mixing of active material with bindrer carbon black on the magnetic stirring.....	34
<b>Figure 3.6:</b> Images shows the the pasting of slury on copper foil by using doctor blade. ....	34
<b>Figure 3.7:</b> Image shows the cutting electrod by using punching machenie.....	35
<b>Figure 3.8:</b> Images shows cutting electrodes and thefavrication and assambly of coin cell in the glove box.....	35

<b>Figure 3.9:</b> Schematic shows the complete assembly of coin cell in inert atmospheres in glow box.....	36
<b>Figure 3.10:</b> The schemamatic of preperation of Hollow carbon spheres with composites. ....	37
<b>Figure 4.1:</b> Schematic shows the XRD of prestine Fe <sub>3</sub> O <sub>4</sub> , NiO, followed by composite Fe <sub>3</sub> O <sub>4</sub> /NiO and Fe <sub>3</sub> O <sub>4</sub> /NiO@HCSs. ....	38
<b>Figure 4.2:</b> Images of the sample pure Fe <sub>3</sub> O <sub>4</sub> , NiO and composite Fe <sub>3</sub> O <sub>4</sub> /NiO @HCS .	40
<b>Figure 4.3:</b> Shows the EDX of prepared samples Fe <sub>3</sub> O <sub>4</sub> , NiO, HCSs, and NiO/ Fe <sub>3</sub> O <sub>4</sub> @HCS ssamples that are prepared. ....	41
<b>Figure 4.4:</b> Figure shows the Ramman spaectrosopy Fe <sub>3</sub> O <sub>4</sub> , NiO, NIO/ Fe <sub>3</sub> O <sub>4</sub> and NiO/ Fe <sub>3</sub> O <sub>4</sub> @HCSs. ....	42
<b>Figure 4.5:</b> Pattern Shows the FTIR of the samples NiO, Fe <sub>3</sub> O <sub>4</sub> , HCSs and composite NiO/ Fe <sub>3</sub> O <sub>4</sub> .....	43
<b>Figure 4.6 (a, b, c, d, e):</b> Shows the XPS of the composite Fe <sub>3</sub> O <sub>4</sub> /NiO@HCSs with plotes given C 1s, O 1s, Fe 2p and Ni 2p and survey respectively.....	45
<b>Figure 4.7:</b> EIS of prestine Fe <sub>3</sub> O <sub>4</sub> , NiO, Fe <sub>3</sub> O <sub>4</sub> /NiO and Fe <sub>3</sub> O <sub>4</sub> /NiO@HCSs and the coulombic efficiency ternery composite.....	46
<b>Figure 4.8:</b> Plotes shows the Cyclic voltametry of prestine Fe <sub>3</sub> O <sub>4</sub> and NiO.....	47
<b>Figure 4.9:</b> Plotes shows the Cyclic voltametry of prestine Fe <sub>3</sub> O <sub>4</sub> and NiO.....	48
<b>Figure 4.10:</b> Schematicshows the five cycles of GCD fro composite Fe <sub>3</sub> O <sub>4</sub> /NiO@HCSs .....	48
<b>Figure 4.11:</b> Schematicshows the Rate capability of prestine Fe <sub>3</sub> O <sub>4</sub> , NiO, Fe <sub>3</sub> O <sub>4</sub> /NiO and Fe <sub>3</sub> O <sub>4</sub> /NiO@HCSs and the coulombic efficiency ternery composite .....	49
One C represents the charging and discharging of lithium-ion battery in one hour, as we see in the above trend increase in C- <b>Figure 4.12:</b> Schematicshows the Rate capability of prestine Fe <sub>3</sub> O <sub>4</sub> , NiO, Fe <sub>3</sub> O <sub>4</sub> /NiO and Fe <sub>3</sub> O <sub>4</sub> /NiO@HCSs and the coulombic effeciency ternery composite.the specific capacitance of electrode .....	49
<b>Figure 4.13:</b> Schematicshows the Rate capability of prestine Fe <sub>3</sub> O <sub>4</sub> , NiO, Fe <sub>3</sub> O <sub>4</sub> /NiO and Fe <sub>3</sub> O <sub>4</sub> /NiO@HCSs and the coulombic effeciency ternery composite .....	50

## LIST OF SYMBOLS, ABBREVIATIONS AND ACRONYMS

LIBs	Lithium-Ion Batteries
SIBs	Sodium-ion Batteries
HCS	Hollow Carbon Spheres
TMOs	Transition Metal Oxides
TMC	Transition Metal Chalcogen
LCO	Lithium Cobalt Oxides
LFP	Lithium iron phosphate
CV	Cyclic Voltameter
EIS	Electrochemical impedance spectroscopy
GCD	Galvanic Charge and Discharge
CV	Cyclic Voltameter

## ABSTRACT

This present work explores the development and electrochemical assessment of a ternary  $\text{Fe}_3\text{O}_4/\text{NiO}@$ HCSs: composite. This composite is synthesized through hydrothermal and thermal treatments to optimize the interface and microstructure of the materials. The unique combination of iron oxides ( $\text{Fe}_3\text{O}_4$ ) and nickel oxide (NiO) with hollow carbon spheres (HCSs) aims to exploit the synergistic effects between these components. The HCSs  $\text{Fe}_3\text{O}_4/\text{NiO}$  composite achieves a remarkable initial discharge capacity of 1623 mAh/g. However, its most notable feature is its stability over prolonged cycling after 1000 cycles at a rate of 0.3C, the composite maintains a robust capacity of 520 mAh/g. In contrast, the pristine  $\text{Fe}_3\text{O}_4$ -NiO anode shows a substantial decline, with its capacity falling below 300 mAh/g at 0.3C. Additionally, impedance measurements reveal that  $\text{Fe}_3\text{O}_4/\text{NiO}@$ HCSs exhibit significantly lower impedance compared to pristine NiO,  $\text{Fe}_3\text{O}_4$  and composite. This reduction in impedance is indicative of enhanced electronic conductivity and improved lithium-ion transport within the composite. The findings highlight the superior performance of  $\text{Fe}_3\text{O}_4/\text{NiO}@$ HCSs.



# CHAPTER 1: INTRODUCTION

## 1.1 Motivation

Due to economic, scientific, and technological development, Planet Earth is dealing with two major Challenges one is energy crises, and the second is global warming, the primely used energy sources are fossil fuels more specifically Oil, coal, and gas meet 85% of the energy demands of mankind[1],[2]. However, fever fossil fuel resources and environmental impact (global warming) limit their usage, and find new alternative ways to overcome the above shortcomings [3]. The journey starts with green energy production, for example wind energy, hydropower, thermal energy, biomass energy, and solar energy. As we know conversion and storage are distinct from each other, this can be connected by electrochemical chemistry. Fuel cells, supercapacitors, and batteries are based on the mechanism of electrochemical mechanisms [4]. Amongst different kinds of energy resources wind energy, hydropower, thermal energy, biomass, etc. batteries are the best-fitted energy conversion and storage device. These batteries mainly consist of an electrolyte (ionic conductor) sandwich between two electrodes Cathode (positive electrode) and Anode (negative electrode), and it works based on redox (oxidation and reduction) reaction.

Batteries have many types for instance Lead acid, Nickle Cadmium, Zinc ion batteries, Podetium ion batteries sodium-ion batteries, etc[5]. However, lithium-ion batteries gain extensive attention due to high Gravimetric and volumetric capacity (more loading within a material), Fast kinetics, long cycle span, and lightweight [6]. Furthermore, lithium-ion batteries do not offer a memory effect while Ni-based and Pb-based batteries have a memory effect, the voltage of Ni-based and Pb-based batteries is three times less than LIBs. In very few years lithium's growing market demands tremendously becoming a powerhouse from phones in our have to every portable electronics. Lithium-ion batteries became a demanding product for electrical and hybrid vehicles, which later came to meet consumer needs by about 50% sail in 2018. In Fig 1.5 we clearly see the market demands of lithium-ion in the market in the last decades. Nevertheless, the low availability results in making it cost-effective, and taking fire is also one major concern for LIB [7] s. In Fig1.1

we clearly observe that lithium-ion batteries have superior specific energy and specific power compared to other types of batteries.

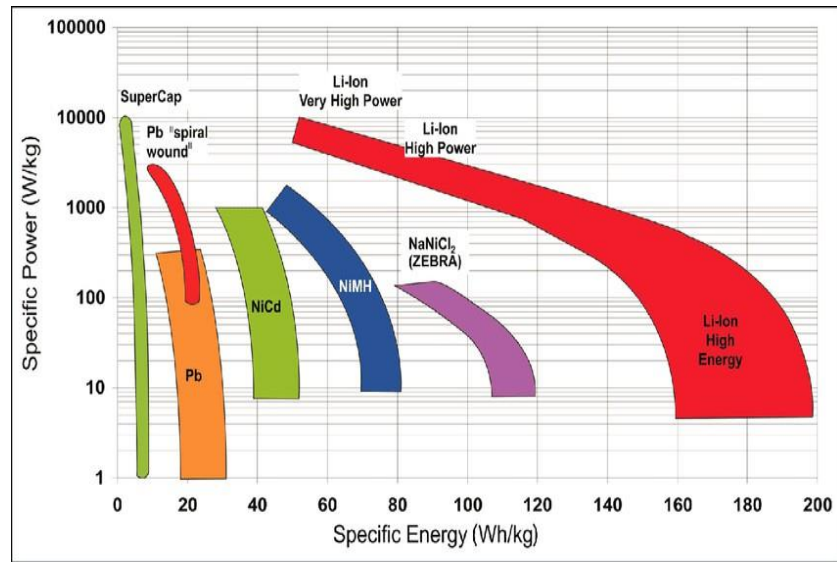


**Figure 1.1:** Ragone plot of different types of batteries technology with different specifications at cell level for the application of automobile.

### 1.1.1 Batteries Verses Supercapacitor Verses Fuel Cell

The electrochemical similarities, two electrodes system, and electrolyte in between transport electrons through the external path and ion flow via electrolyte these three-device work in similar manner. However, they differ in their reaction mechanism, fuel cells direct types convert chemical energy into electrical energy, while supercapacitors and batteries also convert chemical energy into electrochemical, but they are closed systems [8]. The supercapacitor can store charge on the surface of the electrode via an electrostatic double layer this is why supercapacitors have high power density (fast ion and charge diffusion through Charges these materials which is responsible for high energy capacity compared to supercapacitors, in the same way, hybrid supercapacitors become hot point which gives better energy and power density compared to other type supercapacitors. fuel cells are devices that use hydrogen as gas as fuel and produce electric current. The redox mechanism of fuel is we give fuel ( $H_2$ ) on the anode this hydrogen gas converts to  $H^+$  ion (oxidation) through a catalyst which is on the surface of the anode, these ions move through electrolyte

moves toward the cathode and electrons move through external path is Combine with  $H^+$  ion and air (O) to form water at output [9].

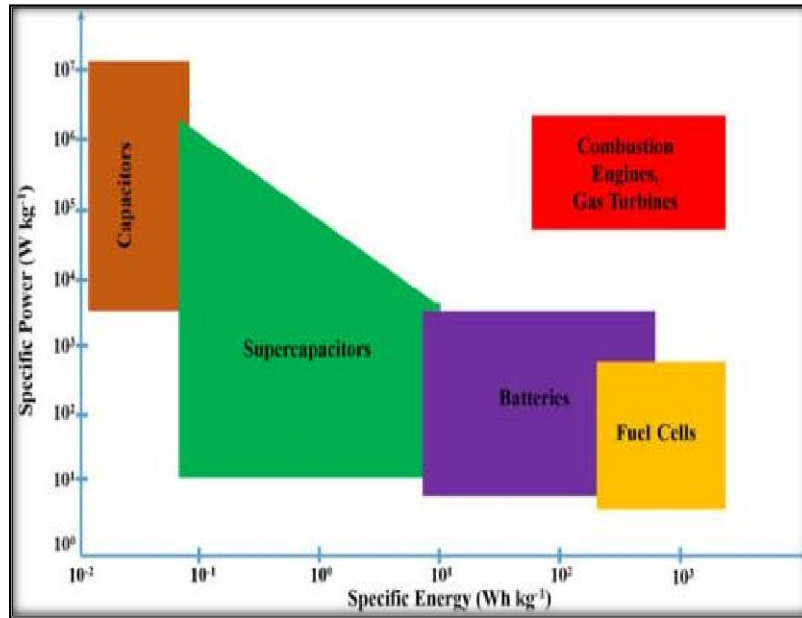


**Figure 1.2:** Ragon plot for Supercapacitor, Fuel cell and batteries against specific Energy density and power density with permission [9]

The energy density of fuel cells is very high compared to batteries and supercapacitors. However, the main issue with this storing mechanism. Because H<sub>2</sub> is lightweight gas we need large enough space to accommodate. This serious issue of storing more hydrogen fuel researchers work on highly porous materials (for example MOFs, Zeolites, and Carbone souse material) [9] which can store more hydrogen fuel and run vehicles and portable electronics. The lithium-ion batteries best fit in device energy density and power density amongst fuel cell and supercapacitor (electrodes) show in the figure1.2, on the other hand, batteries that can be stored.

## 1.2 Lithium-ion Batteries Era

The very first lithium-ion battery was constructed in 1976 at Exxon by Whittingham, he uses the titanium disulfide as cathode material against Lithium as anode. However, his experiment for the commercialization of Lithium-ion batteries ends with bed

results because the Lithium counter electrode formed dendrites formation which result in short-circuiting.

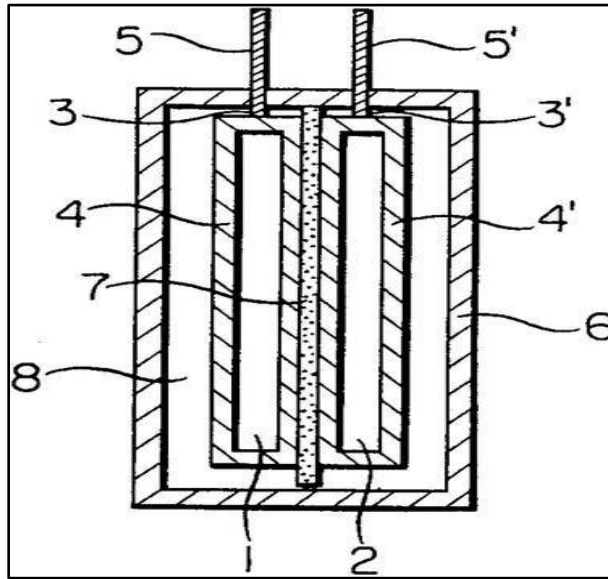


**Figure 1.3:** Shows the first lithium-ion battery pattern By Yohsino, the cathode is  $\text{LiCoO}_2$  against carbon Represent by 1 and 2. The number 3 is current collector, 4 shows the SUS nets, 5 external electrodes Terminal, 6 case, 7 separator, 8 electrolyte [9].

In the same way in 1976 Besenhard was first to observe the reversible intercalation of Lithium ion into Oxide and Graphite used as anode and cathode electrode. Goodenough was first who proposed layered material  $\text{LiCoO}_2$  as cathode with high capacity and potential in 1981 After two years in 1983 Goodenough proposed Manganese based Low-cost spinal structure cathode material gain extensive attention [10]. These anodes like  $\text{LiMO}_2$  have limitations in way of commercialization due to unsafe anode material. In 1987 Yoshino et al, was the first group who  $\text{LiCoO}_2$  and carbonaceous material as cathode and anode material respectively and filed these devices as patent, as these two materials are stable in atmosphere. Yoshino success in safety of lithium-ion batteries by dropping iron lump was the cause and large-scale manufacturing and modern commercialization of Lithium-ion batteries started in early 1990.

### 1.3 Basic of Lithium-ion Batteries

Batteries are electrochemical devices that convert electrical energy into electrical

its mainly categorize in two types, one primary batteries and secondary batteries. The batteries that work in one way means they're not been used after one time, however the batteries that can be used more than once and based on redox are called secondary batteries table 1.1 explain the difference of the above-mentioned batteries.

The working principle is very simple based on redox reaction shows in the figure2, the Lithium-ion batteries consist of positive electrode (cathode) and negative at opposite end (anode) is separated by liquid type gel consist of lithium salt (provide the path for Li ion) and the cathode and anode are separated by a thin porous membrane, which provide Path and allow li ion and block the electron to avoid short circuit this configuration is show in figure 2. Sony was the first commercialization industry to start production of Limbs two decades before a similar configuration was used. The working mechanism is simple by applying force on the cathode, for example like  $\text{LiCoO}_2$  releases lithium ion and electron, the electron goes through external. circuit towards anode while the lithium- ion moves through the electrolyte toward the counter electrode (lithium storing electrode).

**Table 1.1** Shows the basic difference of Primary and secondary batteries.

<b>Ser.</b>	<b>Properties</b>	<b>Secondary Battery</b>	<b>Primary Battery</b>
1.	Recharge-ability	Rechargeable	Non-rechargeable
2.	Maintenance	Well, Maintain	Periodic maintenance
3.	Cost	High	Low
4.	Cycle life	Long	Short
5.	Toxic	No	Yes
6.	Examples	LIBs	Lead acid

On the anodic side LIBs these ions while moving through electrolyte and electrons are combine and same proces in opposite direction in case. The diffusion of ion through the electrolyte faces several challengies regarding layer interfaces where the dendrites form permenently that degrades the life of batteres. So for long cycle life and sustainable lithium ion batteres the uniform and stable solid electrolyte interfacde is our need. The ion diffusion within the material and interfacial kinetics can affect the battereis life. The figure 1.4 shows the basec function of lithium-ion battereis, where the cathode is lithium cobalt Oxide and anode is graphite matererial. The graphite is an intercalating type material where the diffuse from the electrolyte to anode, and these types of materail shows the insertion type of reaction the chances of pulverization is negligible about 0.3%.

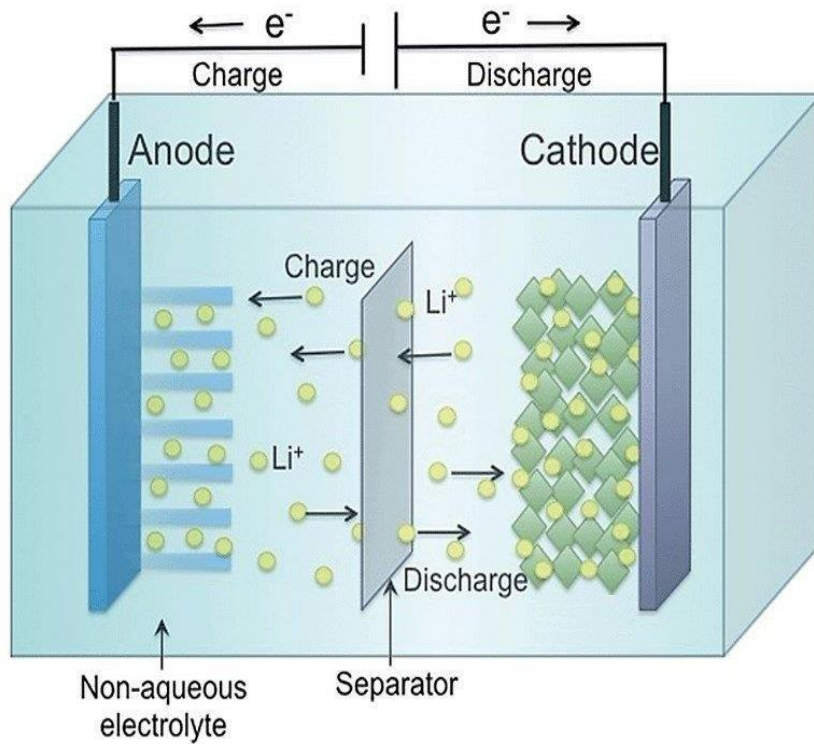


**Figure 1.4:** Schematic illustrate assembly and working mechanism of Lithium-ion batteries.

The electrolyte used in commercializing lithium-ion batteries are lithium-based solutions, facilitating the ion flow from the cathode to anode during the charging. And thin membrane consists of polymer which is also called separator sandwich between electrodes used to hinder the short circuit.

## 1.4 Why Lithium-ion Batteries

The other types of batteries include Lead acid batteries, Nickel cadmium batteries, Nickel metal hydrates batteries, Sodium sulfur batteries Flow batteries are facing challenges. The Lead acid batteries show low energy density, shorter cycle life, poor efficiency and Environmental impact. In the same the Nickel cadmium batteries are having serious issues of memory effect, the element used are toxic and lower energy density. Furthermore, the Nickel metal hydrates, sodium sulfur and flow batteries are hindered due to lower energy density, self-discharge, bulky design, safety concern and cost effective.

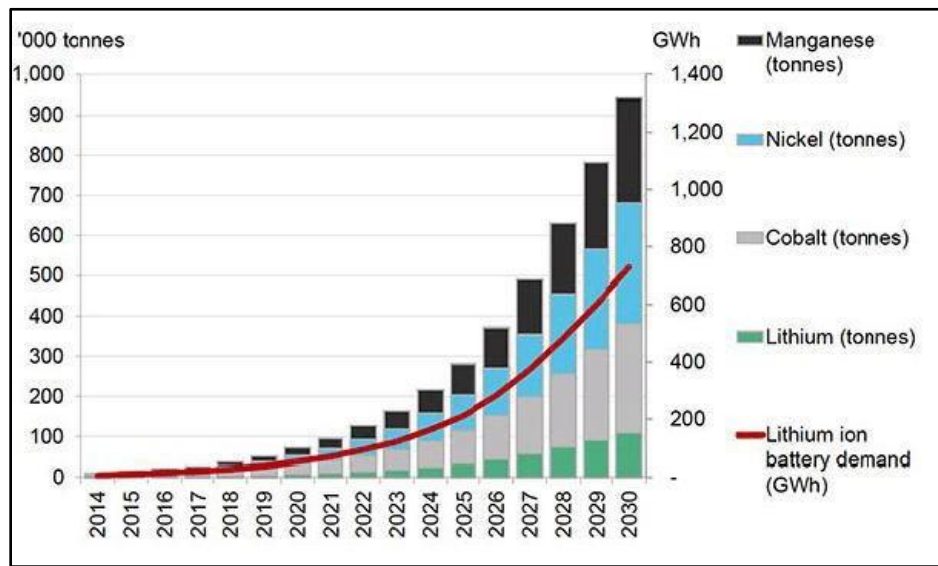


**Figure 1.5:** Trend shows the increasing demands of lithium-ion batteries compared to other types of batteries with time[12].

On the other hand, lithium element in the periodic table, the lithium element is the softest, most reactive, lightest, and least dense form of alkali metal (Group 1). The smaller ionic radius is essential for the ion mobility during intercalation and responsible for high energy density and power density. The lithium ion batteries gains a lot of attiaintion due to cycle life, no memory effec and its light wieght. The ion duffusion within electrod during the charging and discharging proces also called \*Shuttle Chair\* mechanism [11]. because of Li ion moves from lower potential electrode (anode) to higher potential electrode (cathode). Every perticuler material which selected as electrode and reaction happens on

that electrode we determine the total Gibbs free energy change. The Overall reaction and transfer of electron on can estimate their theoretic capacity and voltage. separator use in lithium ion batteries to avoid the short circuiting of batteries. For Fabrication of high-performance sodium ion battery (SIB) you need to understand the two major terms. The first one is energy density which calculates the energy stored contains or fit in size or weight. The energy density comes from the product of specific capacity and output voltage.

$$\mathbf{Energy\ Density} = \mathbf{E} \times \mathbf{Q} \quad : \mathbf{E} = \text{Voltage} \quad \mathbf{Q} = \text{Specific Capacity}$$

$$\mathbf{E} = \mathbf{E}_{cathode} - \mathbf{E}_{anode} = - \frac{\Delta \mathbf{G}}{n\mathbf{F}} \quad (\Delta \mathbf{G} = \text{Change in Gibbs free energy})$$

$$\mathbf{Q} = \frac{n\mathbf{F}}{3.6\mathbf{M}} \quad (n = \text{Number of transfer electrons, F} = \text{Faraday Constant})$$

From the above simple equation, the energy density depends upon the output voltage and specific capacity. The output voltage is the difference between operating voltages of anode and cathode. The potential of sodium is higher than lithium, and specific capacity which is high due to the high number of electrons transfer and low molecular weight. If we take example of phosphorus having three electron transfer per reaction and low molecular giving the theoretical capacity of 2596 mAh/g [12]. The theoretical specific capacitance having unit mAh/g is calculated by the following formula. For example, carbon which stores one lithium ion by six carbon atoms.



The above reaction shows the lithium charging mechanism to calculate,

$$\mathbf{C}_{specific} = \mathbf{372\ mAh/g}$$

The second term is the power density which tells us how quickly the battery gets charge which depends on how fast the ion intercalations and de intercalation happens, we define different type of C rates, for example a battery gets charges at 6C is mean the battery



is in 10 minutes. The batteries have comparatively lower power density than super capacitors, similarly the sodium ion diffusion rate is slow in comparison to lithium.

$$\mathbf{P} = \mathbf{E} \times \mathbf{I} \quad : \mathbf{P} = \text{power density} \quad \mathbf{I} = \text{current}, \quad \mathbf{E} = \text{Exchange}$$

Current

$$\mathbf{I} = i_0 \left[ \exp\left(\frac{\alpha\eta F}{RT}\right) - \exp\left(-\frac{(1-\alpha)\eta F}{RT}\right) \right] \quad \alpha = \text{transfer coefficient}$$

$$i_0 = \frac{RT}{nFR_\alpha} \quad \eta \text{ is the polarization} \quad R \text{ is gas}$$

constant  $\mathbf{T}$  is absolute temperature

$\mathbf{R}_\alpha$  is the charge transfer resistance

From above simple thermodynamic relation the power density with transfer of effective mass and current that implies fast diffusion and better electrical conductivity. Owning increases the reaction sites and reduces the diffusion path for electron / ion. For best performance we need nanomaterial or nanostructure with high specific capacity, high working voltage and high electrically conductive electrode material for Lithium-ion Batteries (LIBs).

Last two decades we see a lot of progress in performance of sodium batteries electrode material, in anode we use organic and inorganic material. The inorganic material use in anode are categorized into three types based on type of reaction during the charging and discharging, either insertion, conversion or alloy reaction. On the other hand, transition metal oxides (TMOs), polyanionic compounds, metal hexacyanometalates, and organic materials are the material studied for cathode in SIB. Most of the anode materials are captivated due to two major issues, the first one is poor electrical conductivity which directly affects the rate performance and second one is volume expansion during the lithiation and / de-lithiation.

In the following figures explore the material that is widely investigated as cathode and anode material for lithium-ion batteries. In the schematic1.6 the different types of cathodes and anodes are placed according to their specific capacity and potential. The specific capacity relates with the property of material to load and de-load the enough

lithium ion within the structure, and the potential is an intrinsic property of material. We can clearly observe that Loading capacity of Sn, Si alloy compound is high enough, however the lithium as electrode has most high specific capacity, but there are pros and cons related with that mentioned material which hinders that commercialization that why graphite with the very low theoretical capacity of 372 mAh/g widely used in our daily life lithium equipment's.

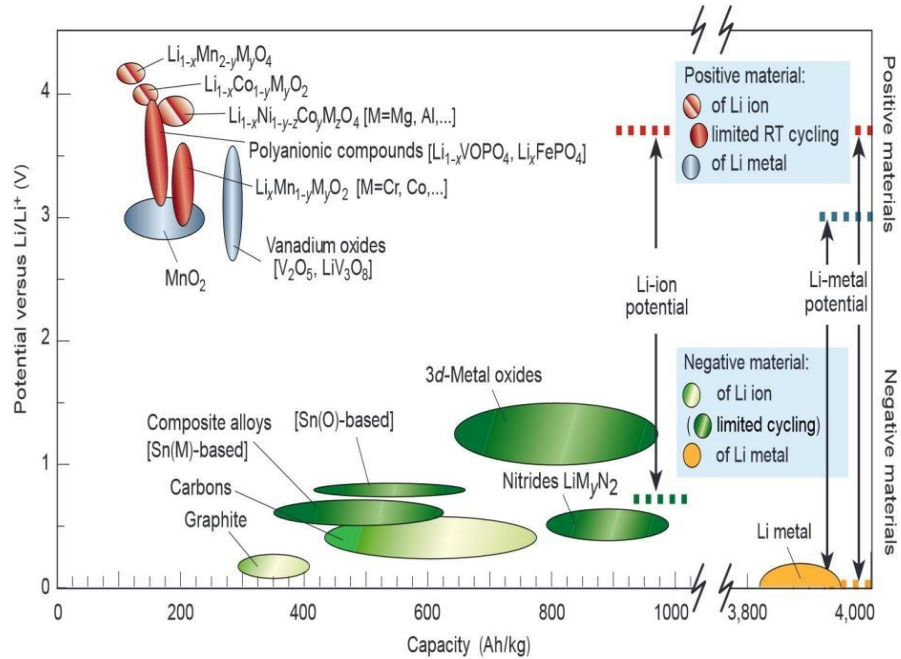


**Figure 1.6:** Schematic shows the investigated material used as anode and cathode for lithium-ion batteries.

The cathode material is facing the main issue of low theoretical capacity which overcomes all energy density of material. We can clearly observe that the voltage of cathode material is high while. on the other hand, voltage of anode is low, secondly the capacity of anode material is high, note that if the gap of potential between cathode material and anode material is high so we different we get is high which means the overall voltage of battery is more enough, which can multiply with specific capacitance of material to give us energy density as a result.

## 1.5 Cathode

One of the key components used as lithium-ion source in lithium-ion batteries is a positive electrode known as cathode. During the discharging the lithium oxidize, electrons are separated moves through external path and ion moves through liquid which is consist of lithium salt and facilitate the ion motion [13]. The working potential cathode is always high compared to anode material. There is no Solid electrolyte formation at cathode however, it may decompose in electrolyte and heat dissipation which further causes thermal runaway to affect the safety of LiBs.

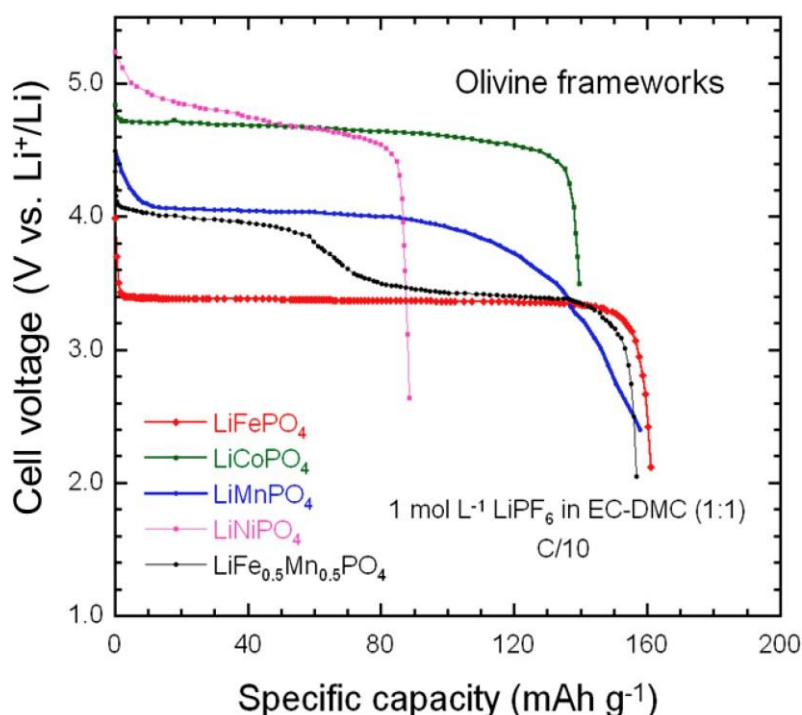


**Figure 1.7:** Shows widely investigated cathode material used in commercialize lithium-ion batteries.

The first cathode used for lithium-ion batteries is LCO called lithium cobalt oxide. Currently there is a commonly used electrode lithium iron phosphate (LiFePO<sub>4</sub>) which is most stable discharging at potential of 3.4 [14]. Similarly, lithium manganese oxide (LMO) has a discharging potential of 4.2 and lithium cobalt oxide with variant ration of nickel and manganese giving high potential and discharge. In addition, other compounds like lithium ion floro-phosphate lithium Vanadium pentoxides, Lithium nickel phosphate is also high

voltage more than 4 and stable discharge specific capacitance, research has continued to find new electrode avoid the issues that cathode face.

## **1.6 Electrolyte**

Batteries improvement towards high capacity while attaining best anode Si based and cathode with high enough discharging and potential, nevertheless organic electrolytes causing safety concern due to its implacable nature. The cathode shows cut off voltage up to 4v because of the interface of cathode and electrolyte, however there are some cathode electrodes which give 5v, but they cross the decomposition threshold of SOA electrolyte. Because of SEI formation art and problem with cathode make more challenging chemistry for single electrolyte to avoid the issues.

As batteries have wide applications, electrolytes need to be drilling well that inferior their flammable nature and withstand 200 C at high temperature [15]. One of the main roles is to make electrolytes reduce the degradation of Solid electrolytes make him resistant to degradation and ionically conductive. The first reported electrolyte for first generation lithium-ion batteries is ethylene Carbonate also known as EC, holding good properties like salt solubility, low vapor pressure, large dipole moment additionally its form robust Solid electrolyte interface. However , it is inferior due to high melting point and high enough viscosity of 1.90 cP at the temperature of 40 C [16]. The second type is called propylene carbonates abbreviated as PC, inhibited due intercalating property within carbonaceous material breaking van der wall forces result in exfoliation of graphite layer. There are many were tries and used as electrolyte like lithium tetrafluoroborate ( $\text{LiBF}_4$ ), Lithium hexafluoro arsenate ( $\text{LiAsF}_6$ ) etc. Currently, electrolyte is lithium hexafluorophosphate ( $\text{LiPF}_6$ ). This electrolyte is highly acidic which facilitates the anion good solubility and shows opposition to reduction and oxidation.

## **1.7 Separator**

A thin membrane used in lithium-ion batteries with very key attributes like allowing the ion flow and resistance to electron flow, separate the two-electrode anode and cathode from short circuit. Which causes safety concerns. Separator physically separates the

contact, and it's made of one layer or two layers of polyethylene or polypropylene type polymer. And make challenges for voltage above then 4v and it can bear the temperature from 135 °C to 165 °C [17].

## 1.8 Anode

Batteries performance is directly dependent on anode material capacity and working potential, the anode material also known as negative electrode its function is store charges during the charging of LIBs. The main drawback of anode material are the first one dendrites formation (needle like structure) which results in direct connection with cathode material and results in short circuits. The second one formation of layer on the surface of anode material also known as solid electrolyte interface, which opposes the ion diffusion within material results in fading capacity and affect over all energy density of lithium-ion batteries [18].

### 1.7.1 Anode Material for Lithium-Ion Batteries

Based on their reaction mechanism we divided the anode material into three types;

- Insertion type materials
- Alloy type materials
- Conversion type materials

### 1.7.2 Insertion type

The Anode material has a very key role in the performance of batteries and is widely investigated due to longer cycle life, high energy capacity and fast charging rate, which means it can affect the performance of LiBs depending on the choice of selected material. In the beginning of commercializing lithium-ion batteries use graphite as anode material with the very less theoretical capacity of 372 mAhg<sup>-1</sup>, However still dominant due to its layer structure which help in the intercalation and deintercalation of the lithium ion during the charging and discharging of battery.

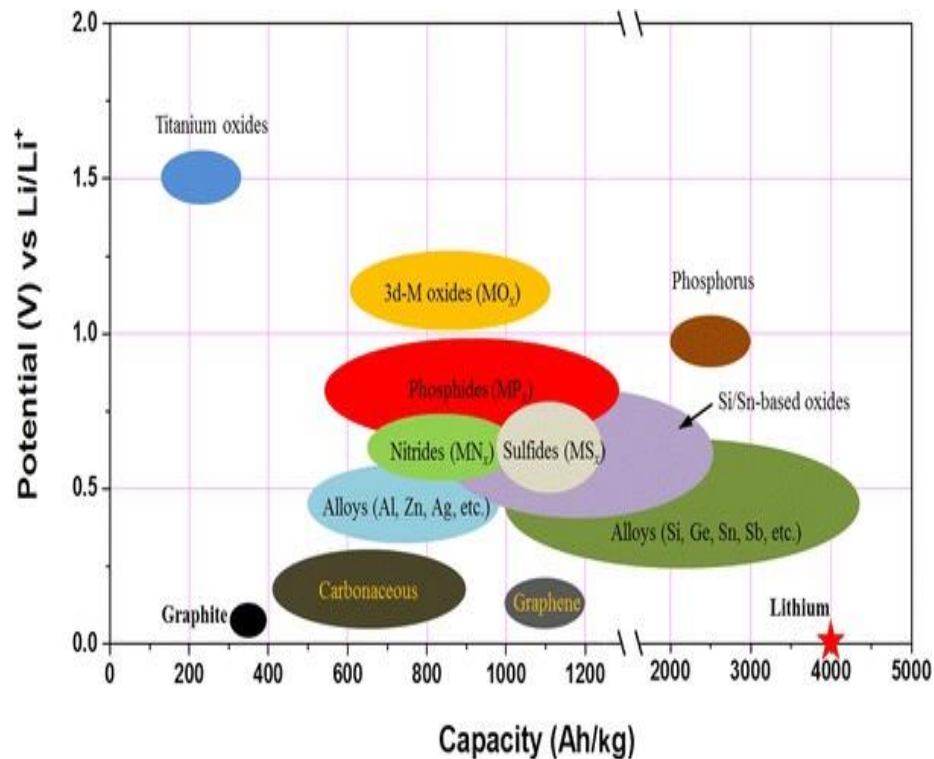


**Figure 1.8:** The Ragone shows the investigated anode material for lithium ion batteries against the capacity and potential.

The graphite materials for application of LIBs, have high cyclic life because of low pulverization (volume change 0.3%) during the charging and discharging. However, due to market demands, graphite doesn't fit because of low theoretical capacity of 372 mAh/g, so therefore Fuji Film introduced a new type of anode TCO alternative to carbon in 1997 but found no space in commercialization due to poor cyclic life. In the same way in 2005 Sony introduced a type of battery with the name of Nexelion as used CSn Co as transition metal composite. The other Si and Germanium have high theoretical specific capacity more than 3000 mAhg<sup>-1</sup> [19].

The issue is material reaction itself, during the lithiation one lithium ion makes bound with six carbons (graphite as anode) and its low working voltage below 0.5 V which is responsible for formation of solid electrolyte interface (SEI) layer on the anode which reduces the overall performance of the anode material, while on the other hand Si atom can store 4 lithium ions which is very high so probability of pulverization in case of Si is high which leads to capacity fading. In the same transition metal becomes a hot point (shows

in Fig 3) which can store two lithium ions and have comparatively less volume expansion of 90% approximately and the theoretical capacity of transition metal oxide is  $700 \text{ mAhg}^{-1}$  to  $1200 \text{ mAhg}^{-1}$  [20].

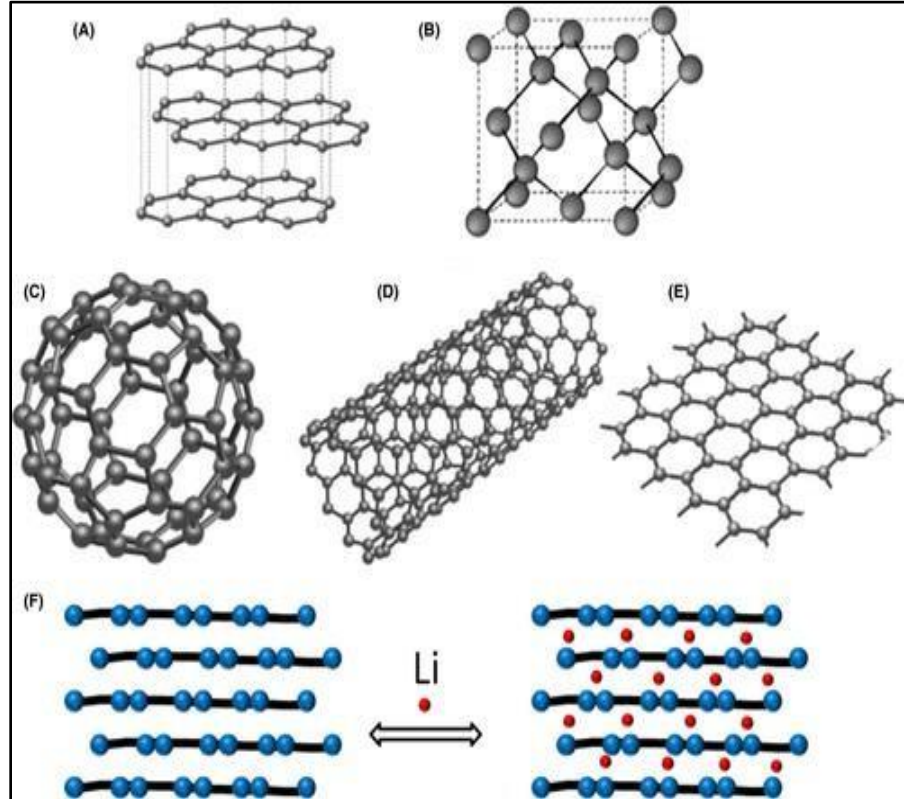


**Figure 1.9:** Schematic illustrate the different type structural carbonaceous materia used for lithium ion batteries [20].

The theoretical specific capacity of graphite and other layered materials like Titanium have been very low, because this material is also called intercalating or insertion type material the lithium ion during charging and discharging do not participate in the reaction with this material they are just adsorb with this type of layered material and the lithium ion between layer is store with sequence also known as stage formation. These storing mechanisms in the carbonaceous in the same as I mentioned before the six carbons as surrounded the one  $\text{Li}^+$  ion so very small deformation in the lattice structure of these carbonaceous types of structure. These graphite structures have amorphous domains linking with one other and it shows the large irreversible capacity after the first cycle and causing fading of capacity of overall. Due to large charge consumptions after first cycle is

responsible for the formation of solid electrolyte interface (SEI) result in decomposition of electrolyte which further reduces the reversibility of Lithium ion [21].

Another common phenomenon happens where some solvents promote the insertion of some molecules from electrolyte with lithium ion in the layer of graphite which high strain due to large volume expansion (approximately 150%) [22], this result in destruction of carbon structure which has been studied widely in research community last decade. This disorder types of carbon material can be synthesis by using a precursor containing carbon material via heat treatment under inert atmosphere. Nevertheless, the mechanism behind the high capacity of these disorder carbon is not fully understood ever large effort has been made. On other hand carbon materials like carbon nanotube (CNT), fullerene, are the following good lithium insertion host material with the optimum layer spacings. The titanium-based lithium-ion batteries, also called Lithium titanium oxides (LTO) have very good lithium reversibility and have good stability. However, this material is inferior due to very low electronic conductivity ( $10^{-13}\text{Scm}^{-1}$ ).

### 1.7.3 Alloy type

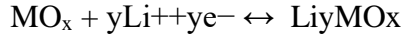
The second class of material which is based on the alloying and dealloying reaction material making these types of reaction are Sb, Ge, Bi, Si and Sn based which have very high theoretical specific capacity up to  $4000\text{mAhg}^{-1}$ . These classes of material are also called alloy type material, is due to constructing alloying and dealloying reaction during the charging and discharging of Li ion. The main issue of these materials is that extreme volume expansion which causes strain and stress in the structure which obviously leads to cracking of particle and capacity fading at the end [23] [23].

TiO<sub>2</sub> shows a better voltage of 1.5 to 1.8 against Lithium, while through research going through the properties of TiO<sub>2</sub> can overcome the issues related with carbonaceous material like dendrite formation, high reversibility due to initial cycle and thermal runaway. Additionally solid electrolyte interface (SEI) layer does not form on the interphase of TiO<sub>2</sub> [24] [24]. This material: found promising place in application of modern demands appliances, as consist of in four different for instance like Brookite, Anatase, Rutile and TiO<sub>2</sub> (B), however the Anatase is widely used.

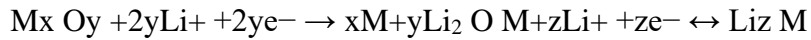


The electrochemical reactions involved on the anodes of LiBs are three types of reaction are listed.

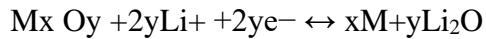
- **Insertion/extraction mechanism”**



- **Li-alloy reaction mechanism:**



- **Conversion reaction mechanism:**



#### 1.7.4 Conversion type

Next class which are from the D block of periodic table known as transition metal combine with chalcogen group element Oxygen to make Transition metal oxide, these materials have high theoretical specific capacity up to  $14 \text{ mAhg}^{-1}$  more than graphite. The transition metal oxide accommodated two lithium ions and the ability to entertain more electrons in the conversion reaction. Transition metal oxides (TMOs) have been abundant in nature and cost effective and nontoxic [25].

This conversion class contains many elements which are widely used for lithium-ion batteries. Among them some elements show exciting behavior and excellent performance interim of Charging and discharging, one of them is iron oxides nano particles which shows excellent theoretical specific capacity of  $915 \text{ mAh/g}$  low cost, non-toxic and easy synthesis. However, faces same issues as volume expansion and poor electrical conductivity [26]. The iron oxide has many types the very first-class iron and oxygen is combined by that ratio of 1 and 1 and form  $\text{FeO}$  or  $\text{Fe}_2\text{O}_2$  called ferrous oxide and when by 2 and 3 ratio called ferric oxide or also called hematite, if they combine ferrous and ferric then it forms  $\text{Fe}_3\text{O}_4$  ferrosferric oxide also known by name of magnetite. And one other type of iron oxide Nanoparticle very famous for Using as radio wave absorption using name of ferrite  $\text{Fe}_2\text{O}_5$ . The material which is widely used for electrochemical devices like Supercapacitor and batteries. These materials have sharp oxidation and reduction behavior while doing Cyclic voltammetry [27], these materials have formed the very uniform Solid Electrolyte interface (SEI) which is Very strong layer form on the surface Of anode

electrode of lithium-ion batteries, this layer can also be confirmed by cyclic voltammetry, this layer is barrier for insertion of electrolyte, avoid the dissolution of electrode into electrolyte.

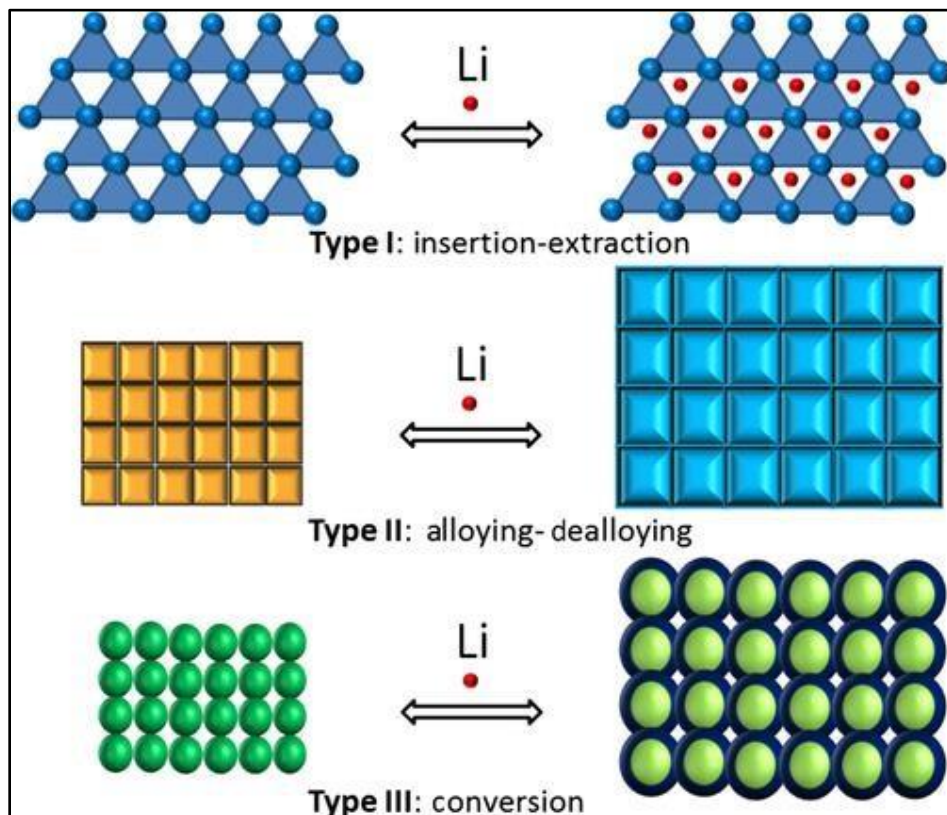


**Figure 1.10:** Schematic shows the structure and reaction mechanism of insertion, alloy and conversion types of materials.

Coming toward the iron oxide the hematite and magnetite are semiconducting composites, which helps in galvanic voltammetry. Nickel Oxide is a good semiconducting oxide material with wide band gap of 3.6 eV use for lithium-ion batteries with theoretical capacity of  $726 \text{ mAhg}^{-1}$  [28] and having better potential against the lithium ion. In this work we synergistically combine  $\text{Fe}_3\text{O}_4$  (magnetite) with nickel oxide to measure their electrochemical performance for lithium-ion batteries.

This composite is prepared by using salts of iron and nickel under certain temperature while maintaining pH has been synthesized. As we mentioned in an earlier paragraph, the transition metal has low electronic conductivity and produces strain during lithiation and dealithiation of ion within crystal, this issue is solved by using various

strategies by different research groups. Carbon is widely popular due to its high conductivity, there are many literatures which use carbon as conductive material for lithium-ion batteries. Among them reduced graphene oxides are widely used as conductive material for application of batteries. Some of the reports have been using carbon nanotubes as conductive source some are multiwall carbon nanotube as conductive; it depends on what you want.

## CHAPTER 2: LITERATURE REVIEW

This chapter includes a detailed description of materials of iron oxides, nickel oxide, hollow carbon spheres and their composite. This chapter will cover all litterateurs that have done specific types of material and different types of morphologies achieved by using different types of strategies.

### 2.1 Iron Oxides

The elements belong to the group of D block of periodic table where the element have half-filled d orbitals are known as transition metal, iron is also part of D block element, the group of periodic containing oxygen, Sulfur, selenium polonium is called chalcogens. When transition metal combines with this group element, they form transition metal chalcogen abbreviated as TMC.

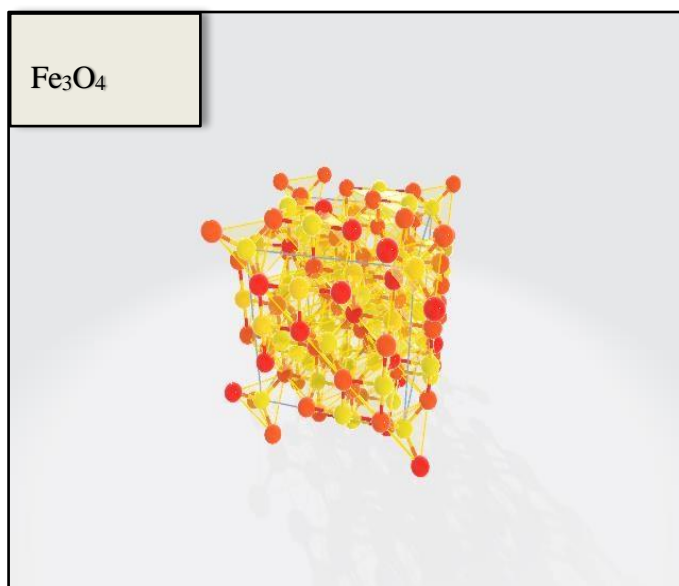


**Figure 2.1** Crystal structure of Fe<sub>3</sub>O<sub>4</sub> genrated from the data base of material project.

There is one class of TMC called TMOs where transition metal combines with oxygen forms transition metal oxides or TMOs, Iron oxide is type of that group. As we know, the valency of transition metal is more than four while the actual valency of Fe is 3 and oxygen is 2. When it forms Fe<sub>2</sub>O<sub>2</sub> so it means its form ferrous oxide by similar ratio of

1:1, and it can also form  $\text{Fe}_2\text{O}_3$  with sharing ratio of 2 and 3 also known as ferric oxide also called Hematite [29]. When we combine ferrous and ferric oxide then its form ferrous ferric oxide also known as magnetite with a sharing ratio 3 and 4 and the formula is  $\text{Fe}_3\text{O}_4$ .

These above two material hematite and magnetite are widely investigated for application of electrochemical devices like batteries and supercapacitor About 926 mAh/g [30] is the theoretical specific capacity of these  $\text{Fe}_3\text{O}_4$  magnetite, the above image shows the cubic crystal formation taken from the library of material project which is an open library for hundreds of materials that have been studied. The  $\text{Fe}_3\text{O}_4$  lattice consists of 56 atoms and can be optimized by using density functional theory. The magnetite is semiconducting material which has about 0.3eV of direct band gap [31].

The  $\text{Fe}_3\text{O}_4$  shows excellent capacity as anode material. Different groups had been studying this material with different types of strategies to improve electrochemical performance. Lim et al, synthesis hollow microspheres of magnetite  $\text{Fe}_3\text{O}_4$  gaining high reversible capacity and cyclic life while using technique of ionic adsorption [32]. Chen et al, also prepared the hollow spheres with mesopores  $\text{Fe}_3\text{O}_4$  attaining specific capacity 500 mAh/g at 0.1 A/g after 50 cycles, as well shows better cyclic stability [33]. Additionally, the  $\text{Fe}_3\text{O}_4$  shows excellent characteristics while making composites with carbonaceous material. Coating magnetite with carbon not only reduces the electrochemical agglomeration, volume expansion but also increases the electronic and ionic diffusion [34], [35]. In the same way Wangs et al, prepared small nano spheres of iron oxide and grow on the surface of graphene sheet showing excellent electrochemical; performance [36].

**Table 2.1** Investigated the  $\text{Fe}_3\text{O}_4$  with Different Strategies and Composite with Carbon.

Strategies	Typical Sample	Electrochemical properties	Ref
Nano structuring	Alpha-Hematite ( $\alpha - \text{Fe}_2\text{O}_3$ )	At 0.2Ah gaining 662 mAh/g after 200 cycles	[37]

	<p>porous hematite (<math>\text{Fe}_2\text{O}_3</math>) nanowires</p> <p>crystalline <math>\text{Fe}_2\text{O}_3</math> grown on Nickel form</p> <p><math>\alpha</math>-<math>\text{Fe}_2\text{O}_3</math> single crystalline nature grown on substrate</p>	<p>At 0.1 c with a specific capacity of 436 mAh/g after 100 cycles</p> <p>At 0.1 C attaining 578 mAh/g after 50 cycles</p> <p>At 0.1C shows 700 mAh/g after 80 cycles</p>	<p>[38]</p> <p>[39]</p> <p>[40]</p>
Hollow structures	<p>Hierarchal subunit of <math>\text{Fe}_2\text{O}_3</math> hollow spheres</p> <p>Micro spheres of Hollow <math>\text{Fe}_3\text{O}_4</math></p> <p><math>\alpha</math> - <math>\text{Fe}_3\text{O}_4</math> with polycrystalline nature</p>	<p>At current of 0.2 Ah attaining capacity of 710 mAh/g after 100 cycles</p> <p>At current density of 200 mAh/g shows capacity of 580 mAh/g after 100 cycles</p> <p>At 0.5 C specific capacity of 1000 mAh/g after 50 cycles</p>	<p>[41]</p> <p>[42]</p> <p>[43]</p>
Carbon coating	<p>Nanospheres of <math>\text{Fe}_3\text{O}_4</math> coating with carbon</p>	<p>At 0.5 C specific capacitance of 530 mAh/g after 80 cycles</p>	<p>[44]</p>

	Fe <sub>3</sub> O <sub>4</sub> nanorod coating with carbon	At current density of 924 mA/g shows 1000 mAh/g after 100 cycles	[45]
	Carbon matrix with nanospheres of Fe <sub>3</sub> O <sub>4</sub>	At current density 200 mA/g shows the specific capacitance of 712 mAh/g after 80 cycles	[46]
Embedding into carbon matrix	Composite of Fe <sub>3</sub> O <sub>4</sub> with carbon forms nanofibers	At current density of 200 mA/g with capacity of 1000 mAh/g After 80 cycles	[47]
	2D hybrid nanosheet of ferrite/carbon	At 100 mA/g it shows capacity of 600 mAh/g after 50 cycles	[48]
	Fe <sub>3</sub> O <sub>4</sub> undirectedly linked with 3D graphene	At current density of 93 mA/g shows excellent specific capacity of 1059 mAh/g after 150 cycles	[49]
	SWCNT interconnected with Fe <sub>3</sub> O <sub>4</sub>	AT 0.5 c shows capacity of 1000 mAh/g after 50 cycles	

## 2.2 Nickel Oxides

Nickle Oxide also comes in the category of translon metal oxide and its wide band gap semiconducting material. Nickel oxide has gained extensive popularity due to its high theoretical capacity of 718 mAhg<sup>-1</sup>, higher density and with additional characteristics like abundance nature, lower cost, and non-toxicity [50] which compares it with commercially

used anode graphite. Moreover, nickel oxide has an intrinsic density of  $6.8 \text{ g/cm}^3$ , while graphite has a density of  $2.26 \text{ g/cm}^3$  which is almost three times less than NiO [51].

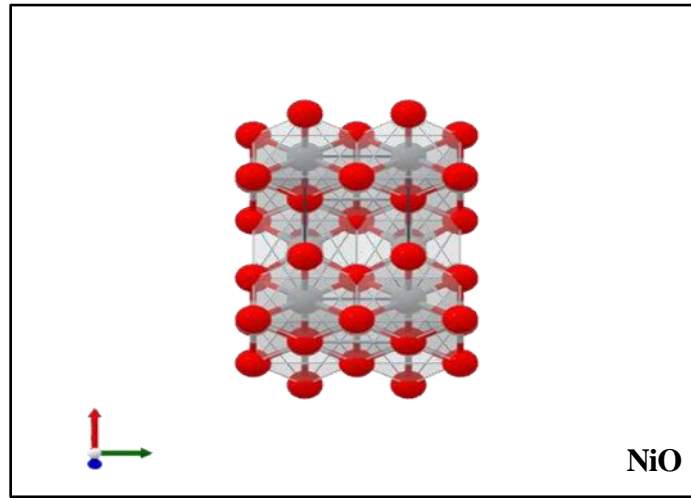


**Figure 2.2:** Plote shows the crystal structure Nickel Oxide which is take out from the material project data.

In the same way, graphite has 5,8 times less theoretical energy density than nickel oxide. During the lithiation the first voltage plateau at 0,6 is the fact for similarly after that during the charging and disc arching, we see the plateau at voltages of 1,3 and 2.2v respectively. Due to its high crystalline and high melting point ( $1453\text{C}$ ), and good ductility [52].is evidence that nickel oxide has better optoelectrical, electrical and magnetic properties. The following figure2.2 shows the nickel Oxide with rhombohedral structure with space group Cmmm [53].

The nickel oxide has a higher density of  $6.8\text{g}$  which is almost three times higher than the commercialize anode material graphite  $2.26 \text{ g}$ . in the same NiO nanoparticles have application for example in solar cell because of its wide band gap around  $3.6 \text{ ev}$  [54]. and widely used in supercapacitors and batteries due to its high theoretical capacity and high reversibility, the nickel gains a lot of attention. Many strategies have been employed while using for application of batteries for example nanorods of nickel oxide, nano tubes, small nanoparticles and different structural engineering to gain high-rate performance, high energy density and cyclic life.



**Table 2.2** Investigated the NiO with Different Strategies and Composite Materials.

<b>Materials</b>	<b>Performnace</b>	<b>Refrence</b>
NiO-C nanocomposite	Shows high intial capacity of 1102 mAh/g and good capacity retention of 37% after 50 cycles	[55]
NiO-C net like structure	Shows stable cyclic performance and better cyclic reversible capacity 430 mAh/g after 40 cycle at current density of 71.8 mA/g with good retainion because of enclotion of carbon	[56]
NiO-C with spherical morphology	The material shows excellent cyclic stability and capacity of 450 mAh/g with excellent coulombic effecience of 68.6% after 100 cycles and shows good effecieincy 0.5 C current rate.	[57]
Nanocomposite of NiO /C	The mateial shows high specific discharge remarkable cyclic stability and capacity of 585.9 mAh/g after 50 cycles with current of 0,5 C	[58]
NiO- C egg like core shell structure	This composite shows high capacity retainion, shows high voltage discharge of 0.22V and high capacity among of 1175.2 mAh/g at the first cycle and retains the capacity 625 mAh/g for 50 cycles.	[59]
	The material shows very large specific discharge of 1400 mAh/g after 50 cycles which is very remarkable and it show hifh rate performance at	[60]

	current density of 0.2 A/g it shows the specific capacity of 1065 mAh/g.	
--	--------------------------------------------------------------------------	--

### 2.3 Hollow carbon spheres

The hollow carbon spheres are a specific class of carbon which shows excellent properties including conductivity, capacity, and rate performance. Hollow carbon spheres (HCSs) are majorly divided into three main types: one is single layer or shell carbon spheres, double shell, and yolk shell. These hollow carbon capsules can be synthesized by different ways: soft template assisted and hard template etc. The hard template synthesis can be while making the spheres of silicon dioxide and growing the carbon on it, then washing out the  $\text{SiO}_2$  using a non-environmentally friendly etching agent sodium hydroxide or hydrofluoric acid (HF) [61]. In most cases, we use silicon dioxide as a hard template for the synthesis of hollow carbon spheres. Herein, in the present work, we also use  $\text{SiO}_2$  as a hard template for the making of HCSs [62]. The hollow carbon spheres consist of single and double bonded carbon atoms.

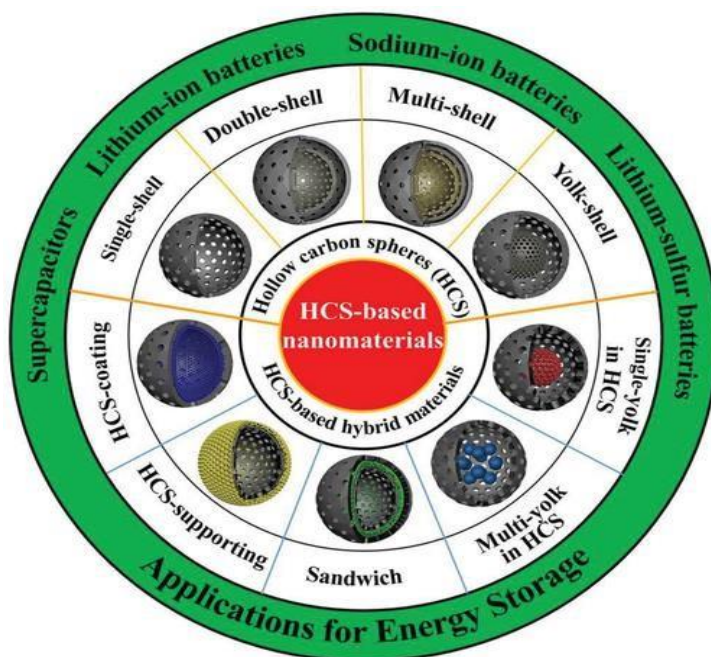


**Figure 2.3:** Schematic illustrate the types of hollow carbon spheres with different types of morphologies used for the application of Energy storage devices.

And these carbon with sp<sup>3</sup> and sp<sup>2</sup> hybridization are elastic and stretch enough to show high performance. These hollow carbon spheres have meso and micro pores which are efficient and suitable for the encapsulation of nanomaterial to be placed inside and this porosity gives them a high surface area which is one promising property. These hollow carbon with different single and double shell are having multiple applications, as shown in the above figure we clearly see that hollow carbon spheres are widely used in supercapacitors, sodium ion batteries, lithium ion batteries and other energy applications [63].

#### 2.4 Fe<sub>3</sub>O<sub>4</sub>/NiO composite

The composite for Fe<sub>3</sub>O<sub>4</sub>/NiO is reported by some journals showing moderate capacity and reversibility however the fading is still a challenge for it. The pulverization and volume expansion are always remain challenges, many groups have studied and try carbonaceous materials to avoid the pulverization issue. And poor electronic conductivity. Zhang et al, synthesis three dimensional Urchin like network ferrous oxide / nickel oxide (Fe<sub>3</sub>O<sub>4</sub>/NiO) as anode electrode for lithium ion batteries, after 100 cycles shows high lithium loading delivering reversible specific capacity of 721 mAh/g at current density of 0.1 A/g [64].

The morphology is essential for their electrochemical performances, Cappong et al, successfully synthesis thin nanosheet with diameter 10-20 nm structure of Fe<sub>3</sub>O<sub>4</sub>/NiO with flower like morphology in the comparison of Pure Fe<sub>3</sub>O<sub>4</sub>, for lithium ion batteries show excellent reversible capacity of 1021 mAh/g [65] after 100 cycles and this discharge capacity was still maintain at capacity of 500 mAh/g showing good coulombic efficiency of 99.6 % and maintain it for 1000 cycles. Qichao et al, prepared core shell structure by hydrogenated TiO<sub>2</sub> with composite of Fe<sub>3</sub>O<sub>4</sub>/NiO as anode material for lithium ion batteries with reversible specific capacitance of 897 mAh/g at current density of 0.2 A/g after 200 cycles. [66] and maintain the specific capacitance of 420 mAh/g after 1000 cycles. Doser et al, successfully prepared Fe<sub>3</sub>O<sub>4</sub>/NiO derived from Fe-MOF and anchored the NiO on it to show high faradic capacitance, shows excellent specific capacitance of 1219 F/g at the current density of 1 A/g and it shows capacity retention after 2000 cycles of 87 % at high current density of 10 A/g. the application is also use for flexible supercapacitor

gain high retention of 83.32 % after 10000 cycles. [67]. In the same way binder plays crucial role in capacity of material and stability of material, because it consists of thin hairlike structure provide elastic strength, Capping et al, solvothermal synthesis the Fe<sub>3</sub>O<sub>4</sub>/NiO heterostructure with spherical flower like morphology to and shows high theoretical capacity and rate performance.

In the present work we exploring the properties of these three upper mentioned metals, we synthesis the composite of iron oxide(Fe<sub>3</sub>O<sub>4</sub>), nickel oxide (NiO) and hollow carbon spheres(HCSs) prepared insitu growth of Fe<sub>3</sub>O<sub>4</sub>/NiO@HCSs. Due the synergistic effect of these three element the material shows excellent behaviour and electrochemical performance. The synthesis of final composite has been done while by the insitu combination of prepared Hollow carbon spheres is mixed with Iron oxide (Fe<sub>3</sub>O<sub>4</sub>) and Nickel oxide NiO. These precursor of iron salt and nickel salt with prepared HCSs actually results in the formation or we can say decoration on HCSs by small particles of iron and nickel nanoparticles.

Nano pores and Nano structure also have advantages of large surface area; However, the low electrical conductivity and low operating potential may result dendrites formation which facilitate the short circuit so safety compromise. On the other hand, soft carbon has layer structure like graphite and store Li ion through the mechanism of insertion and extraction [68]. However, the surface area of soft carbon is small enough that cannot accommodate enough active material. Unfortunately, the graphite is lower in status intern of Li storage, because of low layer spacing. In comparison graphene is widely use in LIBs as composite with active material to enhance the electrochemical properties due to its surface area and high conductivity [69].

Nanocomposites which are based on graphene can not only enhance the upper mentioned properties like electrical conductivity, it also inhibits the pulverization effect (cause die to volume expansion) because of robust framework (structure) [70]. Furthermore, the Nanostructure Based graphene material increases the rate of diffusion by shortening the diffusion path and avoiding the agglomeration effect which can help to

improve the cyclic life and capacity of electrode used in SIB [71]. The literature covers almost all graphene-based Nano composites used for Lithium-ion batteries.

## CHAPTER 3: EXPERIMENTATION

The chapter includes the synthesis of pure Magnetite ( $\text{Fe}_3\text{O}_4$ ), Nickel Oxide ( $\text{NiO}$ ), Hollow carbon spheres, and their composite. This included material is further characterized by different types of tools which will be included in the upcoming chapter, furthermore this material is used as anode material for application of lithium-ion batteries.

### 3.1 Synthesis of NiO

The nickel oxide nanoparticles are prepared by using a coprecipitation method, the required reaction material is nickel nitrate hexahydrate ( $\text{Ni}(\text{NO}_3)_2 \cdot 6\text{H}_2\text{O}$ ) and pallets of NaOH. In the beginning take two clean separate beakers. Make two solutions, in the first beaker take ultra-pure water of 60 ml add 9.3 g of  $\text{Ni}(\text{NO}_3)_2 \cdot 6\text{H}_2\text{O}$  and then stir it vigorously for 30 minutes. In the second beaker take 3 g of NaOH pallets and stir it. Now add alkaline solution drop wise in the beaker containing nickel salt ( $\text{Ni}(\text{NO}_3)_2 \cdot 6\text{H}_2\text{O}$ ). Place it on the stirring for one hour at a temperature of 50 °C. in the last green color precipitates was observed wash several times with DI-water to remove any type of chemical or ionic traces form solution and separate the precipitate by using vitamin paper. Later the product gets dried while placing in the drying oven for 12 h at temperature of 150 °C.



**Figure 3.1:** Image illustrate during the grinding of composite material.

After drying the sample is grinded by using motor and pester for 40 minutes.

In the last sample after a temperature of 300 °C at maple furnace for 2h which results that the color changes from green to black. Before doing further characterization the sample again grinded for 45 minutes to get well powder. The schematic briefly explains the preparation of NiO nanoparticles [72].

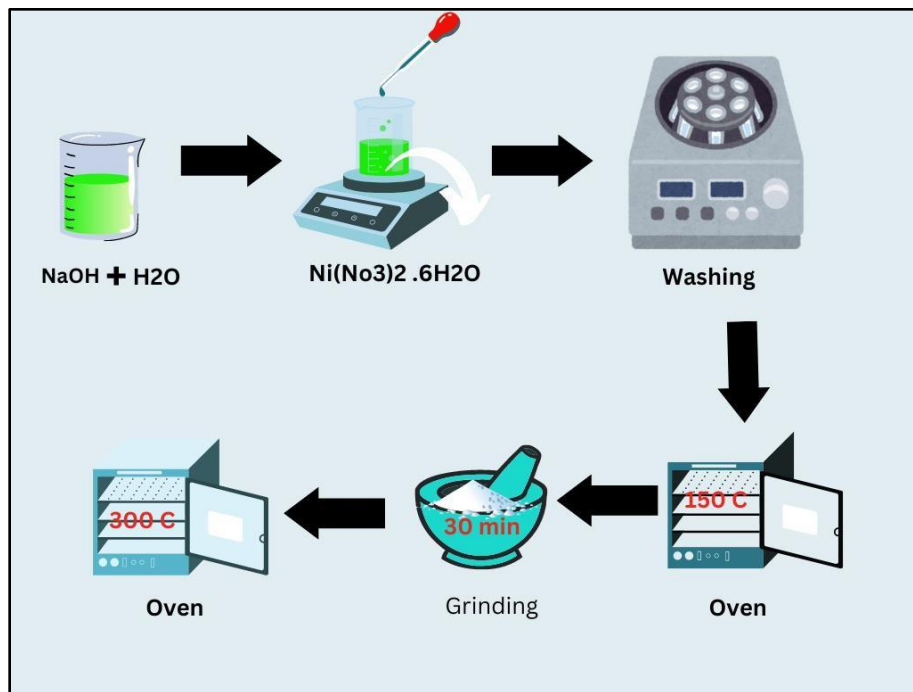


**Figure 3.2:** Schematic shows the step by step synthesis of nickel oxide nanoparticles through co-precipitation method.

### 3.2 Synthesis of Fe<sub>3</sub>O<sub>4</sub>

The nano particles of iron oxide or also known as magnetite is prepared by using the previously reported hydrothermal process. Make a solution containing 0.6 g iron sulfate heptahydrate (FeSO<sub>4</sub>·7H<sub>2</sub>O) and 3.2g NaOH in 40 ml distilled water placed at stirring for 20 min. once the solution was homogenized than transferred to a stainless-steel autoclave, which was place in the drying oven at the temperature of 150 °C for 6 h. Cool down the autoclave at room temperature then wash the product three times with DI-water and one time with ethanol to remove all the impurities from the sample.

At the end the sample is dried in the vacuum oven at the temperature of 40 °C for 18h [73] .

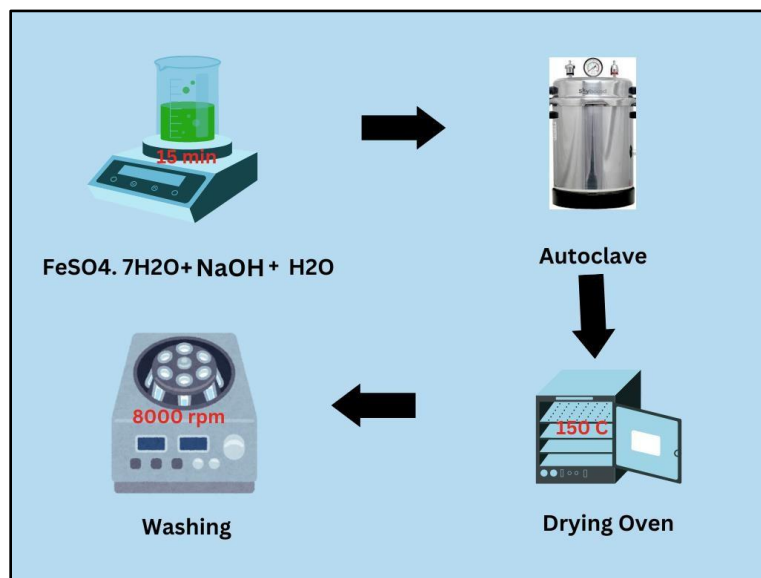


**Figure 3.3:** Schematic shows the preparation step of iron oxides nanoparticles.

### 3.3 Synthesis of Hollow Carbon Spheres

Carbon capsules, also known as Hollow carbon spheres, are prepared via previously reported templated assisted coprecipitation, first make the solution of ethanol and DI-Water by 7:1 (40 ml of water and 280 ml ethanol) the hydrolysis process is far faster than ethanol. And add 12 ml of aqueous Ammonia solution (NH<sub>4</sub> OH 25wt%) to maintain the PH. and place magnetic stirring. Then we add 8,6 g of tetraethyl orthosilicate (TEOS) dropwise in the solution and continue the stirring for a further 30 minutes this stirring is responsible for formation of precipitates (starts nucleation) which further forms silica nanoparticles. In the next step 2.24 ml of Formaldehyde (37wt%) and 1.6 g resorcinol were in the sequence and continued stirring for one complete day at the end of the day we obtained the SiO<sub>2</sub>@SiO<sub>2</sub>@RF brown precipitates which is because of carbon precursor which coated over SiO<sub>2</sub> Nanoparticles.

When carbon precursor coated on the carbon precursor is added these precursors are going into the pores of silica particles which become replica of SiO<sub>2</sub>. After that, we



dried this brown precipitate for 12 h at a temperature of 60°C. The core-shell sample is placed under high temperatures in a Chemical vapor deposition setup under an inert atmosphere to perform carbonization, during this step the uniform carbon layer forms on the surface of SiO<sub>2</sub>. For the last final product, we perform the etching step using hydrofluoric acid to etch the SiO<sub>2</sub> inside of carbon spheres. In this last step the silica nanoparticles are etch from the spheres of carbon, the complete detail of this followed hollow carbon spheres is given below [74].

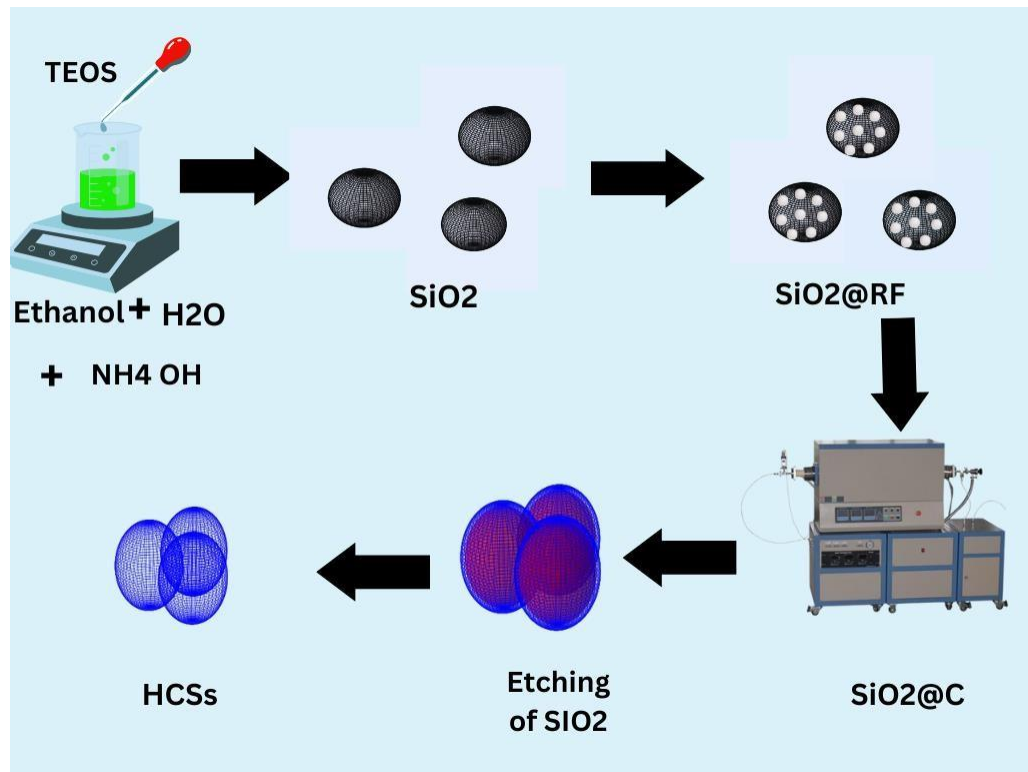


**Figure 3.4:** Schematic show the step by step procedur and effect of ration of ethanol and water effects on hollow carbon spheres.

### 3.6 Fabrication of Coin Cell

This adding includes the preparation of electrodes and assembly of half-cell fabrication.

#### 3.6.1 Slurry Preparation

- The slurry is prepared by using the ratio 70:20:10 of three materials first, we

take 70% of active material, 20% of carbon black (air-like structure), and 10% of PVDF (binder). Then we grind and mix in the motor and pestle.

- Place the material in a clean glass vial, add NMP liquid, and place on vigorous stirring for one complete day.
- The material on copper foil by using a doctor's blade and placed it for drying at room temperature for one day, after that placed in a vacuum oven for more drying.
- Cut the electrode 15 mm from the slurry by using a cramping cutter, then we weigh the electrode.



**Figure 3.5:** Image shows the mixing of active material with binder carbon black on the magnetic stirring.



**Figure 3.6:** Images shows the the pasting of slury on copper foil by using doctor blade.

### 3.6.2 Coin Cell Assembly

- Placed the weighted electrode in the glove box.
- Placed the negative side of the casing, and first place measured electrode.
- Placing the electrode add a drop of electrolyte (containing lithium salt LiPF<sub>6</sub>).
- Place separator (thin membrane conductive for ion and resist electron flow)
- Again, placed the electrolyte and then placed a counter electrode which can be any type of cathode, but I used lithium as the counter electrode.
- After adding the counter electrode, we added a spacer and placed the spring at the end.
- At the end we placed in a cramping machine to form a coin cell.

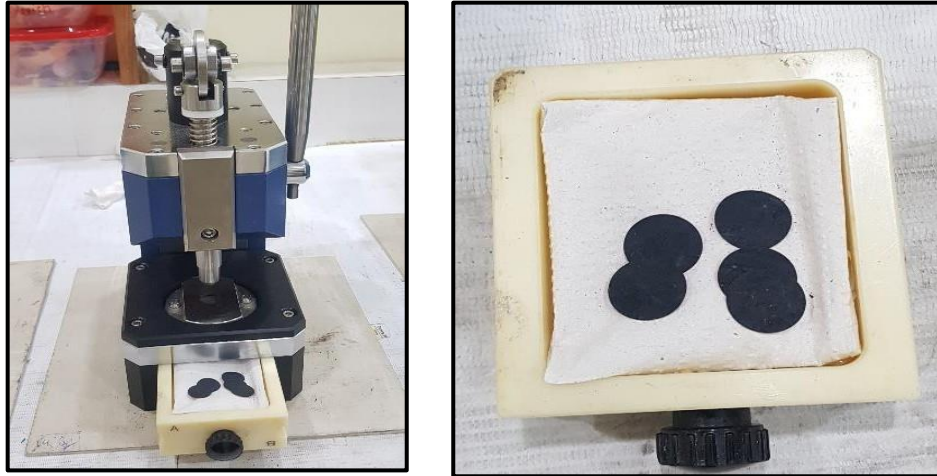


**Figure 3.7:** Image shows the cutting electrode by using punching machine.



**Figure 3.8:** Images shows cutting electrodes and the fabrication and assembly of coin cell in the glove box.

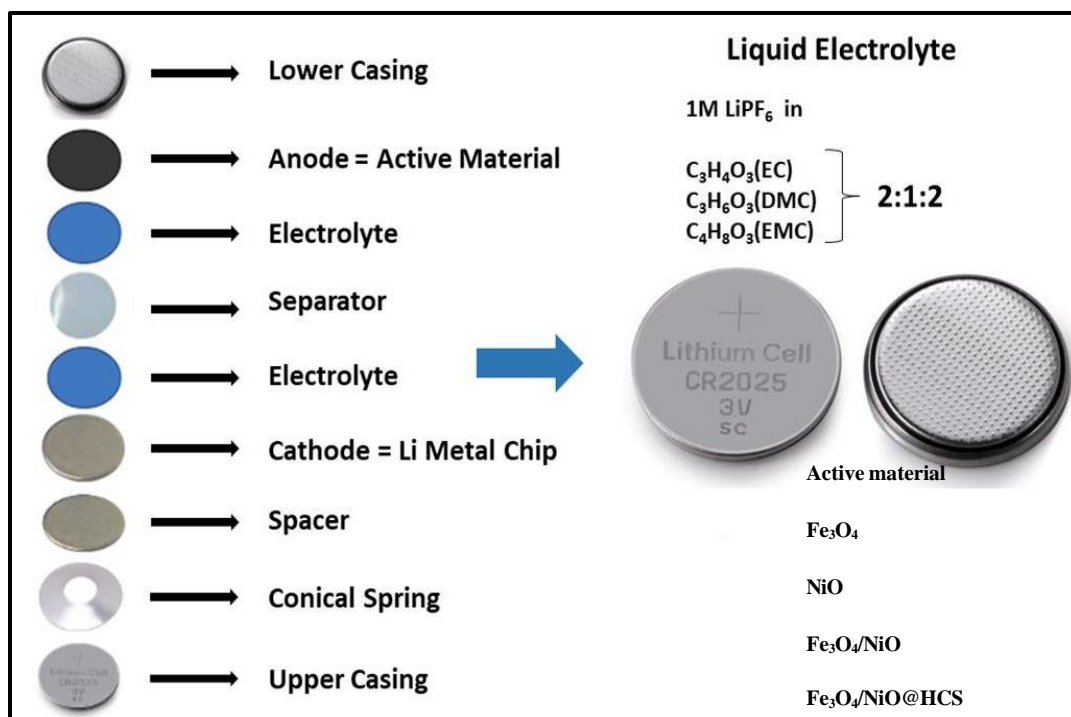


**Figure 3.9:** Schematic shows the complete assembly of coin cell in inert atmospheres in glow box.

### 3.4 Synthesis of Fe<sub>3</sub>O<sub>4</sub>/NiO

The composite synthesis by taking separate beakers 0.1g Nickel acetate tetrahydrate (Ni (ac) .4H<sub>2</sub>O) in 10 ml of ultrapure water and an ultrasonic bath. Take the second beaker place 0.13 g iron sulfate heptahydrate (FeSO<sub>4</sub> .7H<sub>2</sub>O) first dispersed in ultrapure water then we add 0.64 g of sodium hydroxide (NaOH) and continued to mix for 10 minutes. Then we poured the solution into the solution containing nickel solution, again ultrasonicated for 5 minutes and closed the solution in an autoclave with a capacity of 40 ml. This autoclave is placed in over at a temperature of 150°C for 6h. The final product was centrifuged and washed with ethanol and water several times to remove impurities. Then the product was dried at 50°C in a drying oven for 18 h [75].

### 3.5 Synthesis of Fe<sub>3</sub>O<sub>4</sub>/NiO@HCSs

The final product is prepared in situ by using the hydrothermal method, taking three separate beakers, one containing 20 mg of prepared hollow carbon spheres

(HCSs) dispersed in 10 ml of DI-water, the second one containing 40 mg of Nickel salt (Ni (ac). 4H<sub>2</sub>O) disperse in 5 ml of DI-water using ultra sonication bath. The third beaker contained 50 mg of iron sulfate (FeSO<sub>4</sub>. 7H<sub>2</sub>O) dispersed in 5 ml of ultra-pure water, then 250 mg of NaOH was added, and sonicate to disperse in the solution, after that poured the solution of containing iron ions and carbon spheres into nickel-containing solution, and continued centrifugation for 10 minutes.

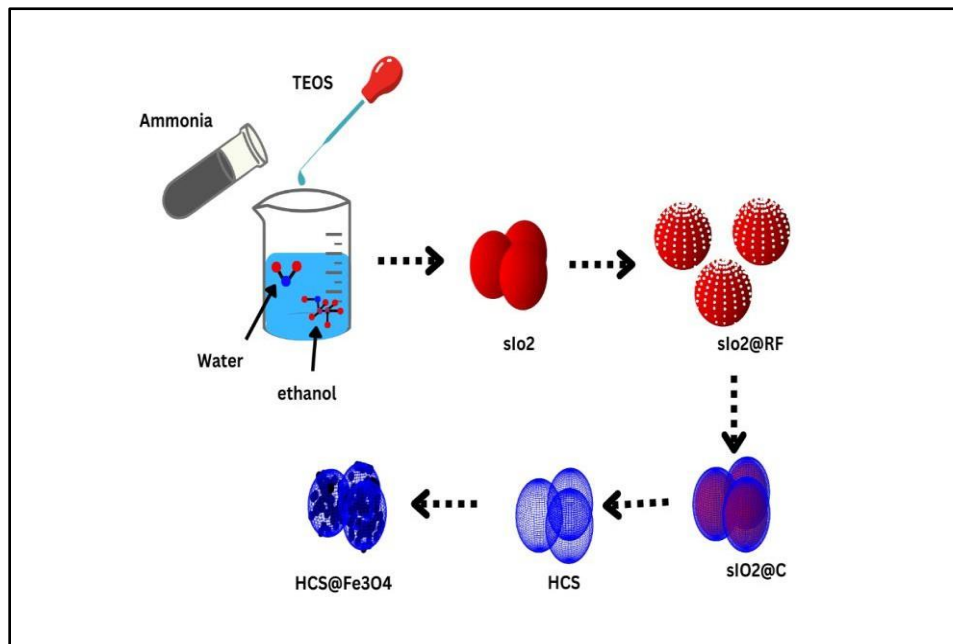


**Figure 3.10:** The schemamatic of preperation of Hollow carbon spheres with composites.

Then pour this solution into a stainless-steel autoclave, and place in the oven at 150°C for 6 h. Next, we collect the black precipitate and centrifuge at 10000 rpm and wash the sample 3 times with ultrapure water, one time with absolute ethanol. The powder product is collected when it is placed for drying at 40°C for 15 h in a vacuum oven.

## CHAPTER 4: RESULTS AND DISCUSSION

The chapter will include all the characterization that we have done for our present work using material, including tool XRD (X- ray diffraction), SEM (scanning electron microscopy), Ramman, FTIR (Fourier transform Infrared spectroscopy), XPS (X- ray photoelectron spectroscopy) and including the application testing like EIS (electrochemical impedance spectroscopy), CV (cyclic voltammetry) and GCD (galvanic charge and discharge).

### 4.1 X-Ray Diffraction (XRD)

X-ray diffraction is a nondestructive technique which is used to analyze the lattice parameter, crystallinity, doping and phase identification. The x-ray beam from the source hit the sample reflect from the Brags plans of sample and constructively interference with one other and results peak at different angle  $2\theta$ .

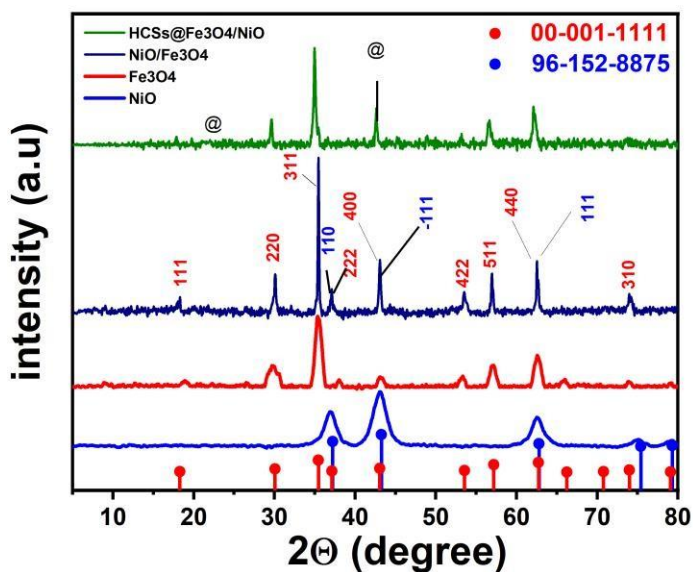


**Figure 4.1:** Schematic shows the XRD of pristine  $\text{Fe}_3\text{O}_4$ , NiO, followed by composite  $\text{Fe}_3\text{O}_4/\text{NiO}$  and  $\text{Fe}_3\text{O}_4/\text{NiO}@$ HCSs.

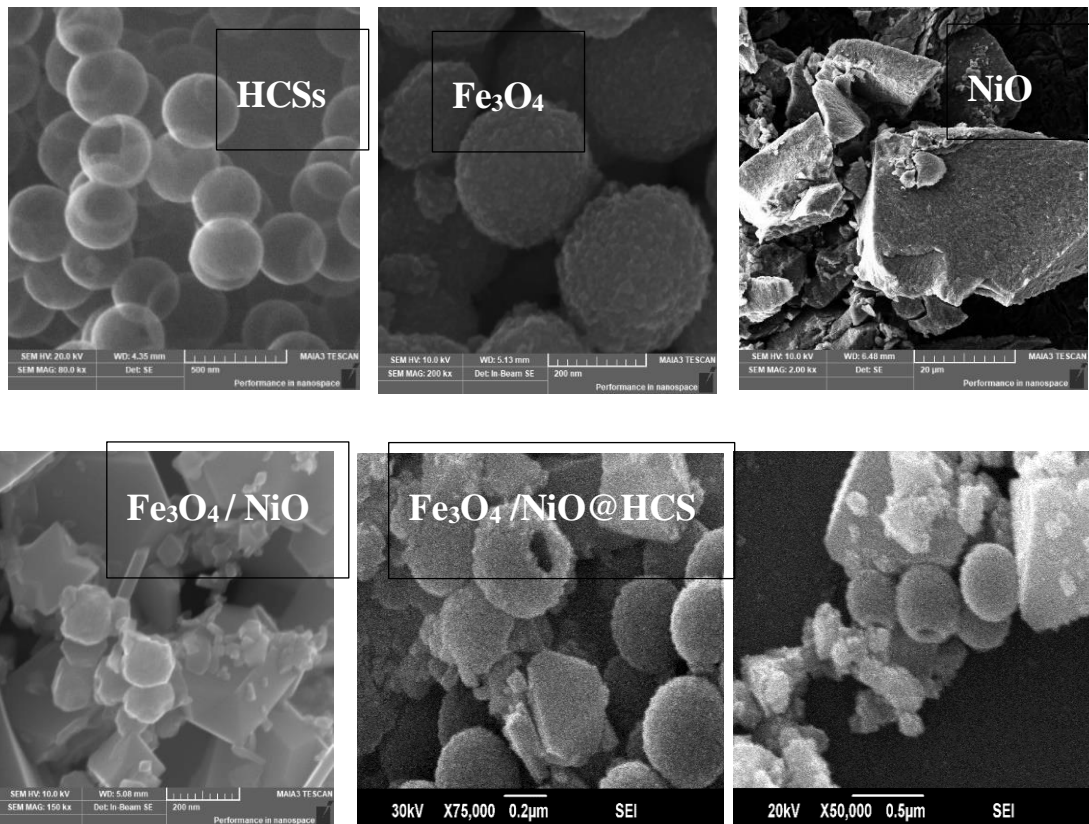
The figure shows the XRD pattern of samples including pristine  $\text{Fe}_3\text{O}_4$ , pristine NiO nanoparticles, the composite of  $\text{Fe}_3\text{O}_4/\text{NiO}$  and composite with hollow carbon spheres.

The peaks in the following pattern on the angle  $2\theta$ , 18, 30, 35, 36, 43, 57, 62 are identification of fine particle formation of  $\text{Fe}_3\text{O}_4$  [76], [77]. that is confirmed by JCPDS card 00-001-1111 and peak at 36, 43, 62 and small peaks at 75 and 79 confirm the formation of crystallin nanoparticles of NiO, which is confirmed by the JCPDS 96-152-8878. Similarly, the well-defined and small intense peaks of composite ( $\text{Fe}_3\text{O}_4/\text{NiO}$ ) indicating the well crystallinity of that composite similarly in ternary composite  $\text{Fe}_3\text{O}_4/\text{NiO}@ \text{HCSs}$  where we see clearly increasing in the peak which indicates the synergistic of carbon iron and nickel. The peak at 43 and small up in the XRD at angle  $2\theta$  25, clearly increases due to hollow carbon spheres presence.

#### **4.2 Scanning Electron Microscopy (SEM)**

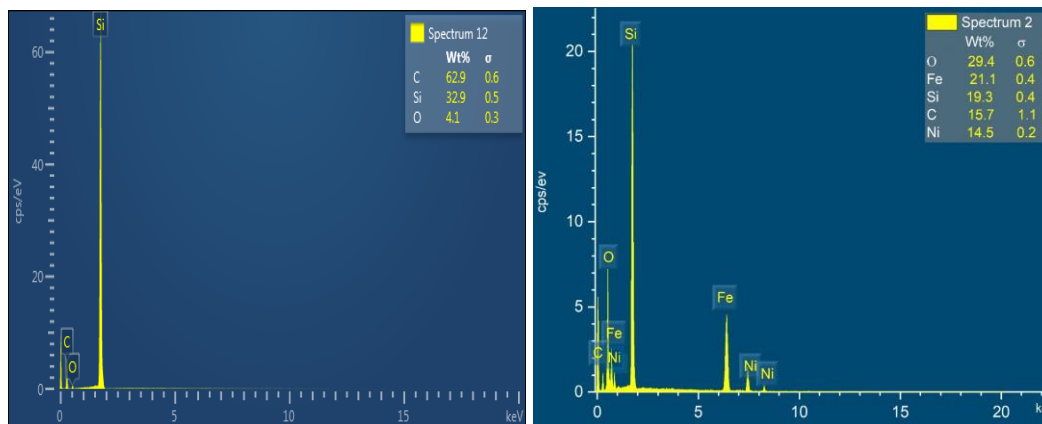
The scanning electron microscopy is also a non- destructive technique which can be used to observe the surface analysis and morphology of the material along with traces of elements present in the sample. The images is taken of the sample by using SEM model JSM-6490A, manufactured by the company of Jeol in Japan. By looking at the images clearly, we observe that hollow carbon spheres are made uniformly around 270 to 290 nm and the purity of these speres is confirmed by using EDX and mapping which is also shown. Iron oxide also forms very well with flowers like morphology. In the next figure we clearly see chunks of material which come with nickel oxide forms cube like structure after the mechanical grinding.

In the next picture we see that iron oxide forms on the surface of these big chunks when we treat both materials by using hydrothermal. In the next two pictures we observe that we grow iron oxide and nickel oxide on the surfaces of carbon spheres. The secondary electron which strikes with surface of material and bounces back these electrons are known as secondary electron which is responsible for identification of elements that are present in the sample. This technique is known as Energy dispersive spectroscopy (EDS) also called EDX. The EDX of final composite clearly confirms the percentage of elements present in the sample. And mapping is used the dispersion of sample presents over certain area that also for quantitative analysis of sample present in the product.



**Figure 4.2:** Images of the sample pure  $\text{Fe}_3\text{O}_4$ ,  $\text{NiO}$  and composite  $\text{Fe}_3\text{O}_4/\text{NiO} @\text{HCS}$

Energy Dispersive X-ray spectroscopy is elemental analyses which measure the quantity of element present in the sample by percentage. The figures clearly indicate that final composite have a high percentage of Oxygen, followed by the percentage of iron, silicon, carbon and nickel respectively.





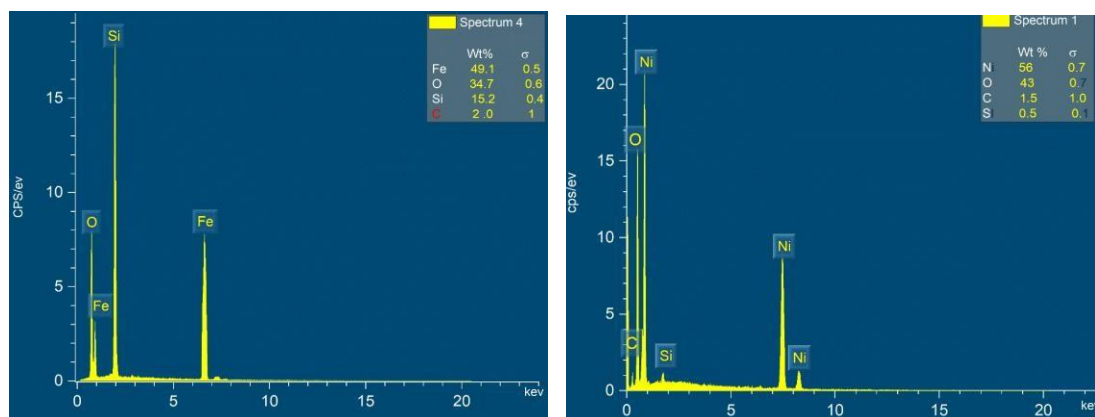


**Figure 4.3:** Shows the EDX of prepared samples  $\text{Fe}_3\text{O}_4$ , NiO, HCSs, and NiO/  $\text{Fe}_3\text{O}_4$  @HCS samples that are prepared.

The carbon percentage is analogous to the large percentage of hollow carbon spheres present in the sample. Similarly, the large percentage of silicon is due to the silico vapor where the sample is placed for scanning electron microscopy.

### 4.3 Raman Spectroscopy

The Raman is nondestructive technique used to analyses the vibrational mode of sample in figure we clearly observe the Raman of all my samples that I have been synthesis. The Raman characterization tool is widely used asymmetric stretches of organic and inorganic compound, and it is also not sensitive to water while the Fourier transform infrared spectroscopy is sensitive to water. At the bottom we observe the different peaks at Wavenumber of 203, 269, 393, 578, and 608 are indicating and contributing the vibrational mode of magnetite ( $\text{Fe}_3\text{O}_4$ ) and the peaks at 363, 534, 702, and 1058 contribute to vibrational mode of NiO, similarly the peaks in final composite are 1357 and 1589 are very dominant and brood which indicate the D- band and G-band of carbon like graphite respectively [78]. The peak 1357 has appeared due to the structural defective that due to Carbon double bound ( $\text{sp}^2$  hybridization) which we see in diamond-like structure and it's also due to irregularity in structure due single bond ( $\text{sp}^3$  hybridization) for instance the graphene like structure. On the other hand, the G band comes due to order Ness in the structure of  $\text{sp}^3$  bonds [76], [77].

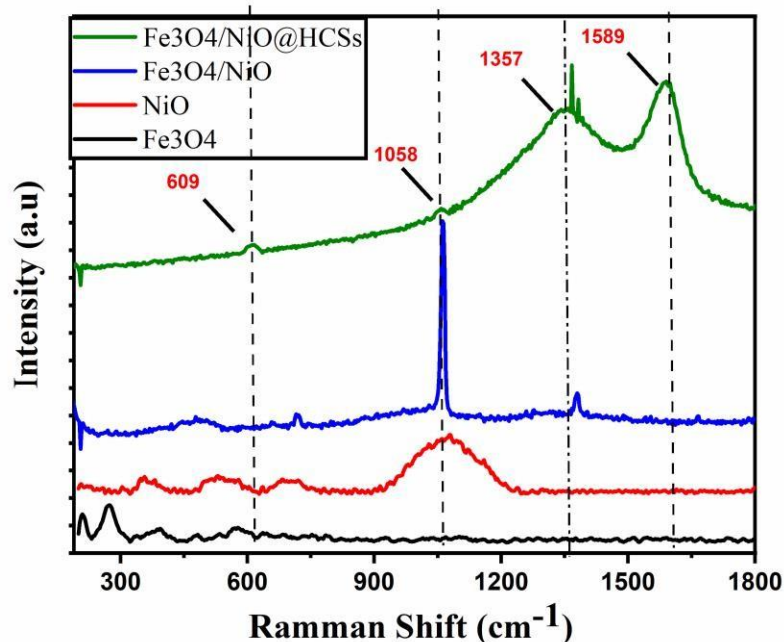


**Figure 4.4:** Figure shows the Ramman spaectroscopy  $\text{Fe}_3\text{O}_4$ , NiO, NIO/  $\text{Fe}_3\text{O}_4$  and NiO/  $\text{Fe}_3\text{O}_4$ @HCSs.

In simple words the hollow carbon spheres form, and it contains defect as well with high crystalline shape. While the peak humps at 608 and 1058 contributing to the formation of NiO and  $\text{Fe}_3\text{O}_4$  with carbon capsule. The ratio of these sharp peaks (D-band and G-band)  $I_d/I_g$  tell us the disorderly in the structure the increase in the ratio of  $I_d/I_g$  indicating that increase in the order and reduce the aromaticity which is due to oxidation of carbon atom with double bonds. In the same way  $I_d/I_g$  increases become 0.7 which indicates the defects increase because of formation of  $\text{Fe}_3\text{O}_4$  and NiO in the structure.

#### 4.4 FTIR Spectroscopy

The Fourier transform infrared spectroscopy is a nondestructive technique used to identify the functional group and identify the traces of another element present in the sample. The molecules and compound have six types of vibration intrinsically, like bending, starching, twisting, waging and two other types, when the infrared ray from source emitted, as we know these above-mentioned types of vibration also comes in infrared regime, so they resonate with source then they constructively appear in output in term of transmittance.

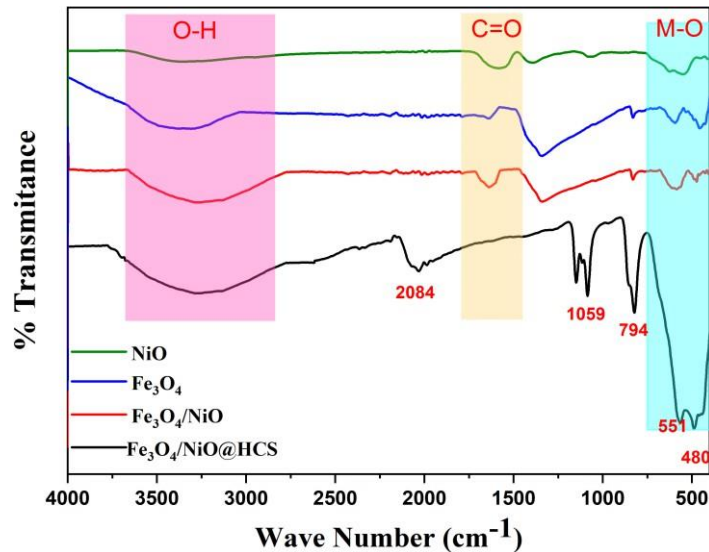


**Figure 4.5:** Pattern Shows the FTIR of the samples NiO, Fe<sub>3</sub>O<sub>4</sub>, HCSs and composite NiO/ Fe<sub>3</sub>O<sub>4</sub>

FTIR is also used to see the molecular and stretching bands, however FTIR is used for symmetric stretches not asymmetric like Raman. Every peak at wavenumber represents the traces of that element. In the figure we clearly see the broad peak from 3000 to 3350 cm<sup>-1</sup>, showing the evidence of hydroxyl group present in the sample. The OH bond is very polar so it appears in the form of a broad peak. Secondly this peak as extra edge of 3400 cm<sup>-1</sup>, which indicate the NH group also present in the sample. Similarly, the peaks at 1621 cm<sup>-1</sup>, 1033, and 503 show the O-H-O bonds present in the sample [78], [79].

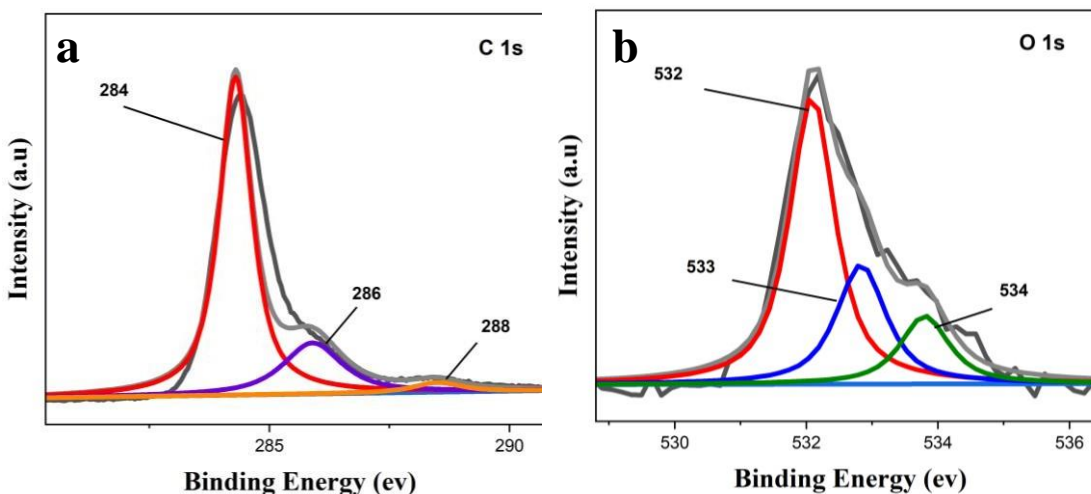
#### 4.5 X-Photoelectron Spectroscopy (XPS)

The x-ray photoelectron spectroscopy is a powerful tool used to analyze surface properties. When x-ray beam hits the surface and emit the photo electron, each of these electrons is having specific binding energy, referred to specific element which can be measured. The x-ray photo electron spectroscopy is widely used for elemental analyses, chemical stat identification and for surface sensitivity.

The elemental analysis as in fig 4.7 shown in the survey data plot where we can easily identify the peak on the specific binding energy to see particular peak of specific element. In the following figure of Fe 2p we see two strong and intense peaks at the binding energy 710.5 ev and 25.4 ev are actually attributed to Fe 2p<sup>1/2</sup> and Fe 2p<sub>3/2</sub> shows that iron

with oxidation of 3 ( $\text{Fe}^{+3}$ ) in Fe 2p which is the evidence of formation of  $\text{Fe}_3\text{O}$ . in the same way two intense and strong peak at the spectrum of Ni 2P at the binding energy of 874.3 and 856.6 ev is associated with Ni  $2p_{1/2}$  and Ni  $2p_{3/2}$ . The peak of Ni  $2P_{1/2}$  at 856.6 corresponds to  $\text{Ni}^{+2}$  and the peak associated with Ni  $2p_{3/2}$  [80] . at binding energy of 874.3 ev is shows the Ni formation when urea is added for optimization of morphology. Furthermore, the peaks in the spectrum of 1s specific binding of 530.4ev are evidence of formation of bounds between oxygen and transition metal either iron or nickel.

Similarly, the peak at 533ev and 532ev indicates the absorbance of water molecules and the adsorption of oxygen on the surface of molecules. in the C 1s [80], [81]. We can observe the peak at 285.2, 286.5 and 289.2ev corresponds to  $\text{sp}^2$  hybridization of  $\text{C}=\text{C}$ ,  $\text{sp}^3$  hybridize carbon-carbon bounds and  $\text{sp}^3$  hybridize carbon oxygen bounding. Similarly, the Survey graph shows the traces of each element present in the sample. The peak at binding energy 287ev indicates that hollow carbon spheres are present in the sample. Furthermore, the sharp and intense peak at the binding energy 529ev shows the oxygen element present, in the same the peak at 726ev and 857ev indication towards the traces of Fe 2p and Ni 2p present in the sample respectively.



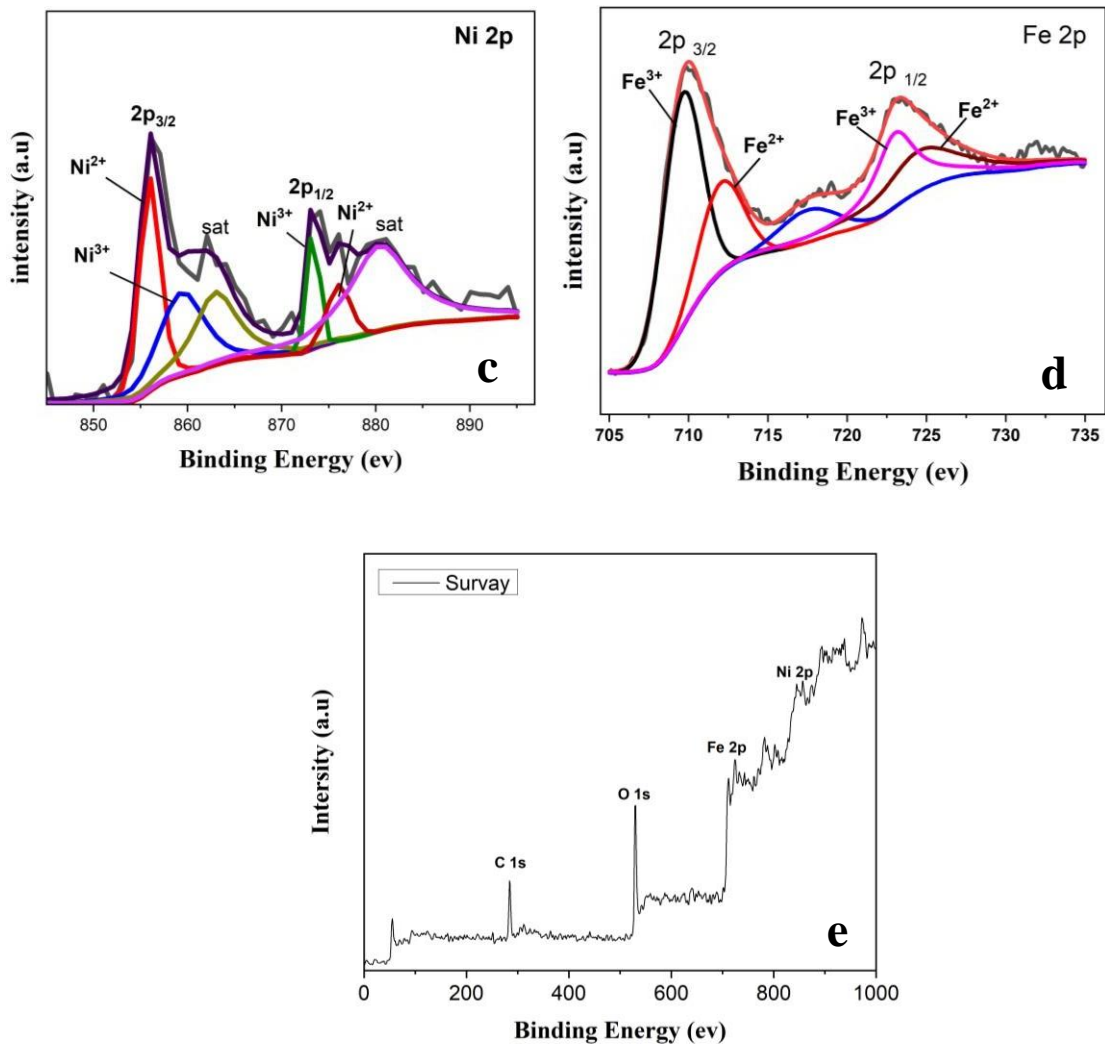


**Figure 4.6 (a, b, c, d, e):** Shows the XPS of the composite  $\text{Fe}_3\text{O}_4/\text{NiO}@$ HCSs with plots given C 1s, O 1s, Fe 2p and Ni 2p and survey respectively.

#### 4.6 Electrochemical Impedance Spectroscopy (EIS)

Electrochemical impedance spectroscopy is a powerful nondestructive technique to measure the equaling series resistance (ESR) of ECs. EIS allows creating models to understand the batteries mechanism system. This electrochemical impedance resistance is a process by which we can measure the resistance of even very complex electrical systems.

Following figure, we see the EIS of the samples iron oxide ( $\text{Fe}_3\text{O}_4$ ), nickel oxide (NiO), their composite along with composite with hollow carbon spheres. . In figure we clearly see that semicircles show resistance, the composite of HCS shows small resistance

about of 50 ohms, it means by adding HCSs enhances the conductivity and in the same way the line after semicircle shows the Warburg of system.

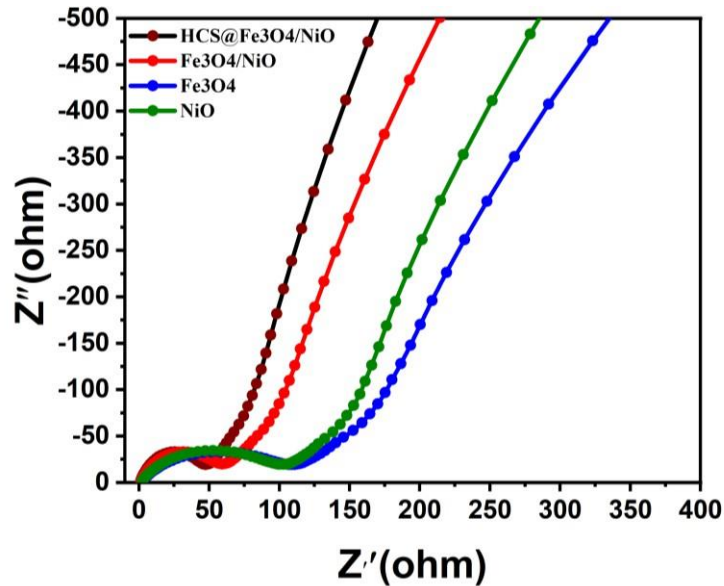


**Figure 4.7:** EIS of pristine Fe<sub>3</sub>O<sub>4</sub>, NiO, Fe<sub>3</sub>O<sub>4</sub>/NiO and Fe<sub>3</sub>O<sub>4</sub>/NiO@HCSs and the coulombic efficiency ternary composite.

This Warburg is attributed to show the diffusion of ion through the electrolyte and anode.

#### 4.7 Cyclic Voltammetry (CV)

Cyclic Voltammetry is a powerful technique used the electrochemistry to investigate the potential of redox (Oxidation and reduction) material. This cyclic voltameter is used for compound identification by their oxidation potential and reduction potential, it can also show the reversibility of redox potential. It uses the counter electrode, reference electrode along with working electrode and ground to the electrochemical properties of specific material. in the first figure we see the CV of magnetite Fe<sub>3</sub>O<sub>4</sub> voltage range from 0 to 3 V shows very sharp and strong peak oxidation and reduction at 1.68 V and 0.65 V respectively [82], [83] . In figure we see 5 cycles, during first cycle very sharp and intense peak appear which is clear indication of formation Solid electrolyte interface in the first cycle die Li<sub>2</sub>O which is due to conversion of Fe<sup>+3</sup>.

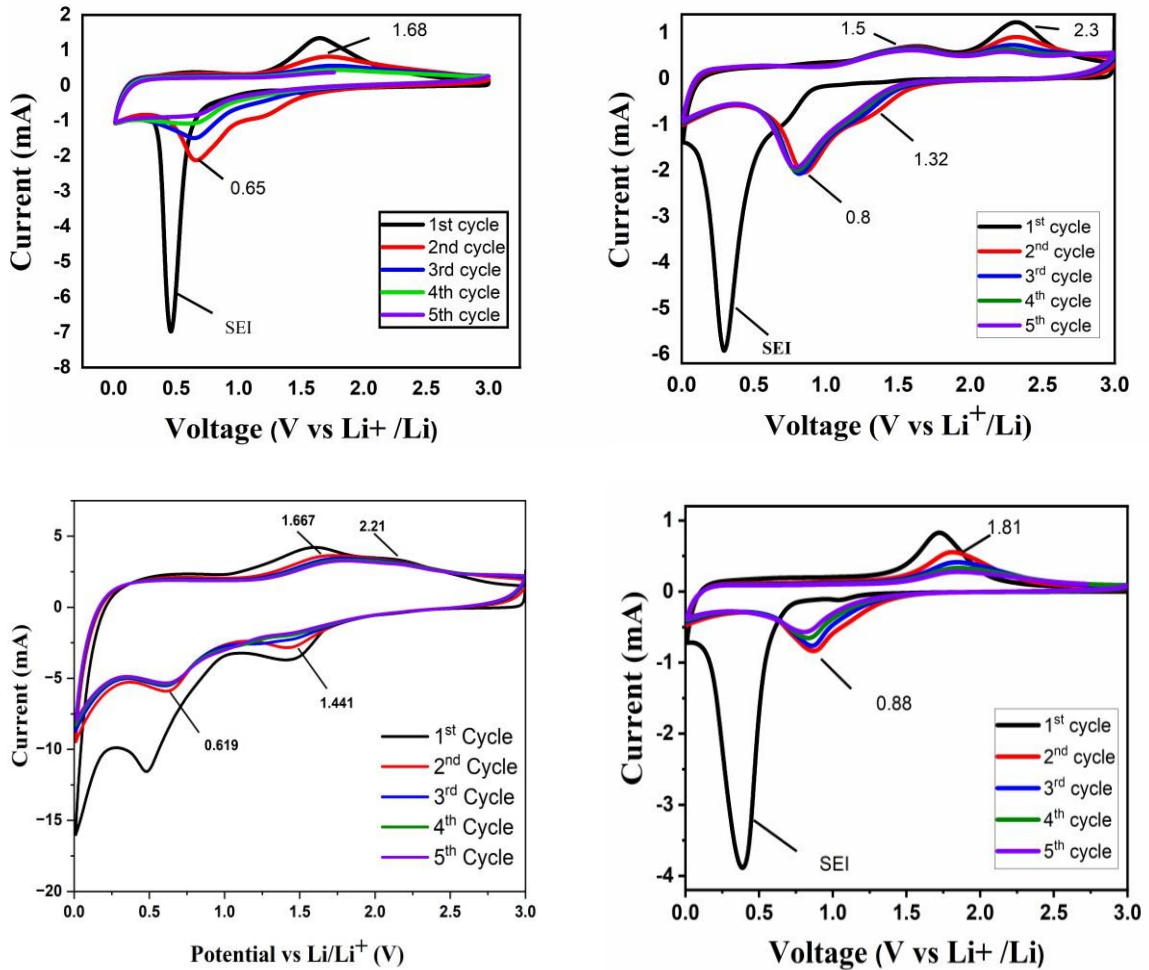


**Figure 4.8:** Plotes shows the Cyclic voltametry of prestine  $\text{Fe}_3\text{O}_4$  and NiO.

The mechanism is  $(\text{Fe}_3\text{O}_4 + 2\text{Li}^+ + 2e^- \rightarrow \text{Li}_2\text{Fe}_3\text{O}_4$  and  $\text{Li}_2\text{Fe}_3\text{O}_4 + 6\text{Li}^+ + 6e^- \rightarrow 3\text{Fe}^0 + 4\text{Li}_2\text{O})$ . Two reduction peaks in curve appeared in the first discharge cycle CV curve of  $\text{Fe}_3\text{O}_4/$  which may be due to the poor conductivity of iron oxide which term in terms of slow conversion of  $\text{Li}_2\text{Fe}_3\text{O}_4$  to  $\text{Fe}^0$  [76, 78]. Similarly, the figure second we see sharp and intense peak at first cycle we are formation of solid electrolyte interface because of  $\text{Li}_2\text{O}$  in reduction of the figure.

In the same the two SEI peak at oxidation which indicates the amorphous formation SEI layer  $\text{Li}_2\text{O}$  and Ni formation. On the other hand, the cyclic voltammety of composite iron oxide shows only one peak at in reduction and one peak at the oxidation. The reduction peak at voltage of 1.8 V clearly indicated hiding behavior of two transition material iron

oxide and nickel oxide. Similarly, we see the sharp and intended peak during the first cycle which is due to formation solid electrolyte interface because of  $\text{Li}_2\text{O}$ . Similarly, this oxidation peak small shoulder due to conversion reactions happens.

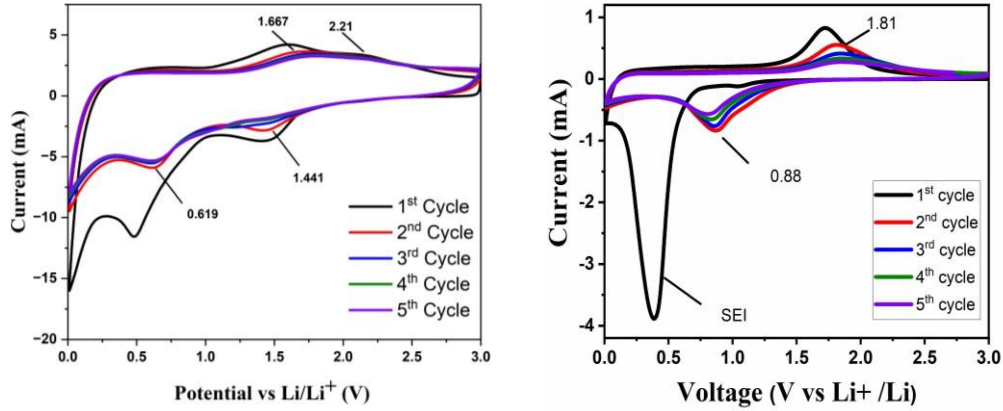


**Figure 4.9:** Plotes shows the Cyclic voltametry of prestine  $\text{Fe}_3\text{O}_4$  and  $\text{NiO}$ .

#### 4.8 Galvanic Charge and Discharging (GCD)

Galvanic charge and discharge (GCD) is a testing technique by which we can measure and observe the charging (loading of lithium ion) and discharging (de-loading of lithium ion) of material. The GCDs test employs measuring the specific capacitance means. Similarly, we observe the peak at voltage of 1.81 [83] which shows the material get oxidized at that voltage, and peak at 0.88 V indicating the material get reduce at the specific voltage.

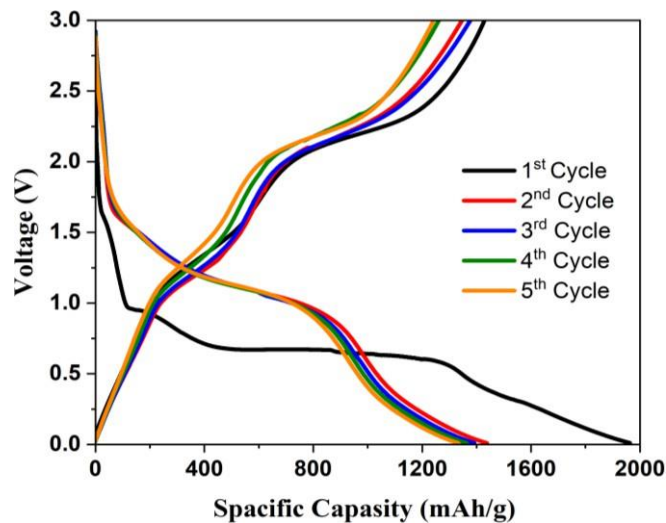


**Figure 4.10:** Schematic shows the five cycles of GCD fro composite  $\text{Fe}_3\text{O}_4/\text{NiO}@HCSs$



The maximum loading of ions in the material, similarly to the GCDs measure the rate capability of material, means to measure the fast diffusion while applying high currents. The specific capacitance is related to energy density and rate capability related to power density.

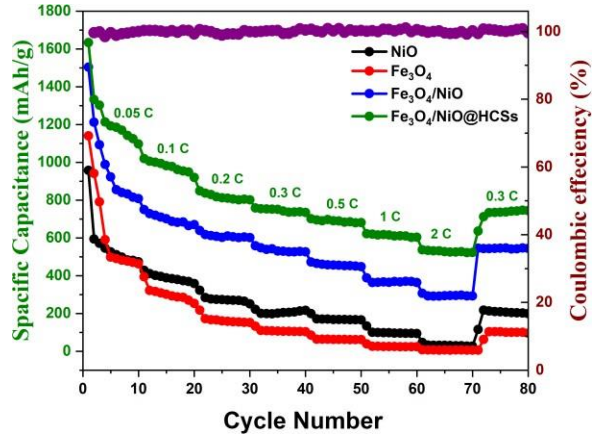


**Figure 4.11:** Schematic shows the Rate capability of pristine  $\text{Fe}_3\text{O}_4$ ,  $\text{NiO}$ ,  $\text{Fe}_3\text{O}_4/\text{NiO}$  and  $\text{Fe}_3\text{O}_4/\text{NiO}@HCSs$  and the coulombic efficiency ternary composite.

Herein in the above we observe five cycles of the charging and discharging of the final sample, in which we see the first discharging of material is about 1963 mAh/g and discharging about 1530 mAh/g [82], [83].

The rate capability shows how fast the battery can charge and discharge, the trend shows the GCD of electrodes  $\text{Fe}_3\text{O}_4$ ,  $\text{NiO}$ ,  $\text{Fe}_3\text{O}_4/\text{NiO}$  and  $\text{Fe}_3\text{O}_4/\text{NiO}@HCS$  with different C - rate along the coulombic efficiency C- rate along the coulombic efficiency.

One C represents the charging and discharging of lithium-ion battery in one hour, as we see in the above trend increase in C- **Figure 4.12:** Schematic shows the Rate capability of pristine  $\text{Fe}_3\text{O}_4$ ,  $\text{NiO}$ ,  $\text{Fe}_3\text{O}_4/\text{NiO}$  and  $\text{Fe}_3\text{O}_4/\text{NiO}@HCSs$  and the coulombic efficiency ternary composite. the specific capacitance of electrode.

Schematic shows the Rate capability of pristine  $\text{Fe}_3\text{O}_4$ ,  $\text{NiO}$ ,  $\text{Fe}_3\text{O}_4/\text{NiO}$  and  $\text{Fe}_3\text{O}_4/\text{NiO}@HCSs$  and the coulombic efficiency ternary composite rate up to 2C (means charging and discharging in 30 minutes) the stress increase on electrode which decreases lithium-ion battery in one hour, as we see in the above trend increase in C-rate up to 2C

(means charging and discharging in 30 minutes) the stress increase on electrode which decreases the specific capacitance of electrode. The above trend shows the coulombic efficiency, The coulombic efficiency is 99.5% of final composite  $\text{Fe}_3\text{O}_4/\text{NiO}@H\text{CSs}$ , which comes when we take ratio of discharge and charge and multiply with 100. The coulombic efficiency tells us the reversibility of ion and electron during charge and discharge. The figure shows the cyclic stability of ternary composite  $\text{Fe}_3\text{O}_4/\text{NiO}@H\text{CS}$ , in trend we observe the specific capacity decreases to certain level which is due electrode degradation [84].

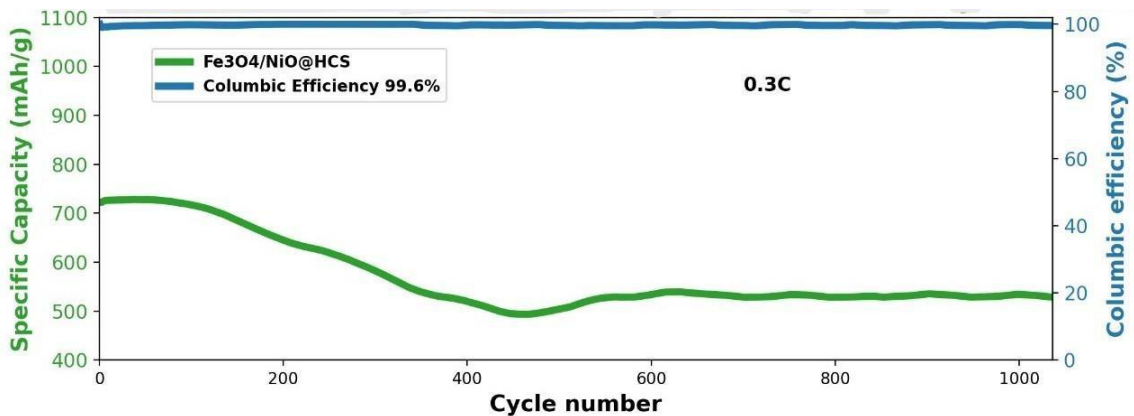


**Figure 4.13:** Schematic shows the Rate capability of pristine  $\text{Fe}_3\text{O}_4$ ,  $\text{NiO}$ ,  $\text{Fe}_3\text{O}_4/\text{NiO}$  and  $\text{Fe}_3\text{O}_4/\text{NiO}@H\text{CSs}$  and the coulombic efficiency ternary composite.

The above figure shows the cyclic stability of ternary composite  $\text{Fe}_3\text{O}_4/\text{NiO}@H\text{CS}$ , in trend we observe the specific capacity decreases to certain level which is due electrode degradation [84]. The specific capacity is stable at 520 mAh/g after 1000 cycles and shows high reversibility of lithium-ion performance with coulombic efficiency of 99.6% after 1000 cycles. This indicates that hollow carbon spheres with micro pores provided high surface area within addition the hollow cage is responsible for absorption high strain energy from the transition metal oxides.

## CHAPTER 5: CONCLUSIONS

### 5.1 Conclusions

Herein, we synthesis ternary composite of  $\text{Fe}_3\text{O}_4/\text{NiO}@\text{HCS}$  via simple hydrothermal method along with comparison of Bare  $\text{Fe}_3\text{O}_4$ , (which were prepared by hydrothermal) and NiO (by co-precipitation method) as well with their composite.in addition uniform Hollow carbon spheres has synthesis via hard templet assisted co-precipitation method with mesoporous structure, the  $\text{Fe}_3\text{O}_4$  show excellent capacity 200 mAh/g after 300 cycles at current density of 300 mA/g. similarly the NiO shows good specific capacity of 2000 mAhg<sup>-1</sup> at first cycle. And shows capacity of 180j after 300 cycles. composite of iron oxide and nickel oxide uniformly decorated on the porous surface of carbon capsules and shows the very well electrochemical performance showing high reversible theoretical specific capacity of 450 mAhg<sup>-1</sup> at current density of 300 mAh/g after 1000 cycles. The rate performance and capacity retention and columbic efficiency of 96% after 600 cycles. This type of structural design and ternary composite can further modify to make better potential anode material for lithium-ion batteries.

## REFERENCES

1. I. Dincer and C. Acar, "A review on clean energy solutions for better sustainability," Apr. 01, 2015, *John Wiley and Sons Ltd.* doi: 10.1002/er.3329.
- [2] V. Kumar, R. L. Shrivastava, and S. P. Untawale, "Solar Energy: Review of Potential Green & Clean Energy for Coastal and Offshore Applications," *Aquat Procedia*, vol. 4, pp. 473–480, 2015, doi: 10.1016/j.aqpro.2015.02.062.
- [3] S. Jebaraj and S. Iniyan, "A review of energy models," Aug. 2006. doi: 10.1016/j.rser.2004.09.004.
- [4] F. Schipper and D. Aurbach, "A brief review: Past, present and future of lithium ion batteries," *Russian Journal of Electrochemistry*, vol. 52, no. 12, pp. 1095–1121, Dec. 2016, doi: 10.1134/S1023193516120120.
- [5] M. S. Whittingham, "Lithium batteries and cathode materials," *Chem Rev*, vol. 104, no. 10, pp. 4271–4301, Oct. 2004, doi: 10.1021/cr020731c.
- [6] J. Wen, Y. Yu, and C. Chen, "A review on lithium-ion batteries safety issues: Existing problems and possible solutions," Sep. 2012. doi: 10.1166/mex.2012.1075.
- [7] M. Winter and R. J. Brodd, "What are batteries, fuel cells, and supercapacitors?," *Chem Rev*, vol. 104, no. 10, pp. 4245–4269, Oct. 2004, doi: 10.1021/cr020730k.
- [8] O. Z. Sharaf and M. F. Orhan, "An overview of fuel cell technology: Fundamentals and applications," Apr. 2014. doi: 10.1016/j.rser.2014.01.012.
- [9] B. Scrosati, "History of lithium batteries," Jul. 2011. doi: 10.1007/s10008-011-1386-8.
- [10] R. Marom, S. F. Amalraj, N. Leifer, D. Jacob, and D. Aurbach, "A review of advanced and practical lithium battery materials," *J Mater Chem*, vol. 21, no. 27, pp. 9938–9954, Jul. 2011, doi: 10.1039/c0jm04225k.
- [11] L. Wang *et al.*, "Nano-structured phosphorus composite as high-capacity anode materials for lithium batteries," *Angewandte Chemie - International Edition*, vol. 51, no. 36, pp. 9034–9037, Sep. 2012, doi: 10.1002/anie.201204591.
- [12] Y. Zhang *et al.*, "Advances in new cathode material LiFePO<sub>4</sub> for lithium-ion batteries," Aug. 2012. doi: 10.1016/j.synthmet.2012.04.025.
- [13] Y. K. Sun, S. T. Myung, B. C. Park, J. Prakash, I. Belharouak, and K. Amine, "High-energy cathode material for long-life and safe lithium batteries," *Nat Mater*, vol. 8, no. 4, pp. 320–324, 2009, doi: 10.1038/nmat2418.
- [14] R. Marom, S. F. Amalraj, N. Leifer, D. Jacob, and D. Aurbach, "A review of advanced and practical lithium battery materials," *J Mater Chem*, vol. 21, no. 27, pp. 9938–9954, Jul. 2011, doi: 10.1039/c0jm04225k.

- [15] M. Nie and B. L. Lucht, "Role of Lithium Salt on Solid Electrolyte Interface (SEI) Formation and Structure in Lithium Ion Batteries," *J Electrochem Soc*, vol. 161, no. 6, pp. A1001–A1006, 2014, doi: 10.1149/2.054406jes.
- [16] S. Shui Zhang, "An unique lithium salt for the improved electrolyte of Li-ion battery," *Electrochem commun*, vol. 8, no. 9, pp. 1423–1428, Sep. 2006, doi: 10.1016/j.elecom.2006.06.016.
- [17] L. Zhang, X. Li, M. Yang, and W. Chen, "High-safety separators for lithium-ion batteries and sodium-ion batteries: advances and perspective," Oct. 01, 2021, *Elsevier B.V.* doi: 10.1016/j.ensm.2021.06.033.
- [18] H. Chang, Y.-R. Wu, X. Han, and T.-F. Yi, "Recent developments in advanced anode materials for lithium-ion batteries," *Energy Materials*, vol. 1, no. 1, p. 100003, 2022, doi: 10.20517/energymater.2021.02.
- [19] Y. Cheng *et al.*, "SnSe/r-GO Composite with Enhanced Pseudocapacitance as a High-Performance Anode for Li-Ion Batteries," *ACS Sustain Chem Eng*, vol. 7, no. 9, pp. 8637–8646, May 2019, doi: 10.1021/acssuschemeng.9b00441.
- [20] Y. Yao *et al.*, "Interconnected silicon hollow nanospheres for lithium-ion battery anodes with long cycle life," *Nano Lett*, vol. 11, no. 7, pp. 2949–2954, Jul. 2011, doi: 10.1021/nl201470j.
- [21] C. Zhu, Y. Zhang, Z. Ma, Y. Zhu, and L. Li, "Mesoporous-Si embedded and anchored by hierarchical Sn nano-particles as promising anode for lithium-ion batteries," *J Alloys Compd*, vol. 832, Aug. 2020, doi: 10.1016/j.jallcom.2020.154935.
- [22] X. L. Wu, Y. G. Guo, and L. J. Wan, "Rational design of anode materials based on group IVA elements (Si, Ge, and Sn) for lithium-ion batteries," Sep. 2013. doi: 10.1002/asia.201300279.
- [23] D. Yang, J. Shi, J. Shi, and H. Yang, "Simple synthesis of Si/Sn@C-G anodes with enhanced electrochemical properties for Li-ion batteries," *Electrochim Acta*, vol. 259, pp. 1081–1088, Jan. 2018, doi: 10.1016/j.electacta.2017.10.117.
- [24] Y. X. Fu, Y. Dai, X. Y. Pei, S. S. Lyu, Y. Heng, and D. C. Mo, "TiO<sub>2</sub> nanorods anchor on reduced graphene oxide (R-TiO<sub>2</sub>/rGO) composite as anode for high performance lithium-ion batteries," *Appl Surf Sci*, vol. 497, Dec. 2019, doi: 10.1016/j.apsusc.2019.143553.
- [25] Y. H. Shi *et al.*, "Fe<sub>3</sub>O<sub>4</sub> nanoflakes-RGO composites: A high rate anode material for lithium-ion batteries," *Appl Surf Sci*, vol. 511, May 2020, doi: 10.1016/j.apsusc.2020.145465.
- [26] M. Zhang, M. Jia, and Y. Jin, "Fe<sub>3</sub>O<sub>4</sub>/reduced graphene oxide nanocomposite as high performance anode for lithium ion batteries," *Appl Surf Sci*, vol. 261, pp. 298–305, Nov. 2012, doi: 10.1016/j.apsusc.2012.08.004.

- [27] X. H. Huang, J. P. Tu, C. Q. Zhang, and F. Zhou, "Hollow microspheres of NiO as anode materials for lithium-ion batteries," *Electrochim Acta*, vol. 55, no. 28, pp. 8981–8985, Dec. 2010, doi: 10.1016/j.electacta.2010.08.039.
- [28] L. Li *et al.*, "Ultra small and highly dispersed Fe<sub>3</sub>O<sub>4</sub> nanoparticles anchored on reduced graphene for supercapacitor application," *Electrochim Acta*, vol. 190, pp. 566–573, Feb. 2016, doi: 10.1016/j.electacta.2015.12.137.
- [29] Y. Wei, B. Han, X. Hu, Y. Lin, X. Wang, and X. Deng, "Synthesis of Fe<sub>3</sub>O<sub>4</sub> nanoparticles and their magnetic properties," in *Procedia Engineering*, Elsevier Ltd, 2012, pp. 632–637. doi: 10.1016/j.proeng.2011.12.498.
- [30] G. Zhou *et al.*, "Graphene-wrapped Fe<sub>3</sub>O<sub>4</sub> anode material with improved reversible capacity and cyclic stability for lithium ion batteries," *Chemistry of Materials*, vol. 22, no. 18, pp. 5306–5313, Sep. 2010, doi: 10.1021/cm101532x.
- [31] W. M. Zhang, X. L. Wu, J. S. Hu, Y. G. Guo, and L. J. Wan, "Carbon coated Fe<sub>3</sub>O<sub>4</sub> nanospindles as a superior anode material for lithium-ion batteries," *Adv Funct Mater*, vol. 18, no. 24, pp. 3941–3946, Dec. 2008, doi: 10.1002/adfm.200801386.
- [32] Z. Zeng, H. Zhao, J. Wang, P. Lv, T. Zhang, and Q. Xia, "Nanostructured Fe<sub>3</sub>O<sub>4</sub>@C as anode material for lithium-ion batteries," *J Power Sources*, vol. 248, pp. 15–21, 2014, doi: 10.1016/j.jpowsour.2013.09.063.
- [33] M. Ershadi, M. Javanbakht, Z. Kiaei, H. Torkzaban, S. A. Mozaffari, and F. B. Ajdari, "A patent landscape on Fe<sub>3</sub>O<sub>4</sub>/graphene-based nanocomposites in Lithium-Ion Batteries," Feb. 01, 2022, *Elsevier Ltd*. doi: 10.1016/j.est.2021.103924.
- [34] J. S. Chen, T. Zhu, X. H. Yang, H. G. Yang, and X. W. Lou, "Top-down fabrication of  $\alpha$ -Fe<sub>2</sub>O<sub>3</sub> single-crystal nanodiscs and microparticles with tunable porosity for largely improved lithium storage properties," *J Am Chem Soc*, vol. 132, no. 38, pp. 13162–13164, Sep. 2010, doi: 10.1021/ja1060438.
- [35] D. Lei *et al.*, " $\alpha$ -Fe<sub>2</sub>O<sub>3</sub> nanowall arrays: Hydrothermal preparation, growth mechanism and excellent rate performances for lithium ion batteries," *Nanoscale*, vol. 4, no. 11, pp. 3422–3426, Jun. 2012, doi: 10.1039/c2nr30482a.
- [36] D. Lei *et al.*, " $\alpha$ -Fe<sub>2</sub>O<sub>3</sub> nanowall arrays: Hydrothermal preparation, growth mechanism and excellent rate performances for lithium ion batteries," *Nanoscale*, vol. 4, no. 11, pp. 3422–3426, Jun. 2012, doi: 10.1039/c2nr30482a.
- [37] Y. Han *et al.*, "Preparation and electrochemical performance of flower-like hematite for lithium-ion batteries," *Electrochim Acta*, vol. 56, no. 9, pp. 3175–3181, Mar. 2011, doi: 10.1016/j.electacta.2011.01.057.
- [38] M. A. Rahman, R. Radhakrishnan, and R. Gopalakrishnan, "Structural, optical, magnetic and antibacterial properties of Nd doped NiO nanoparticles prepared by co-precipitation method," Apr. 25, 2018, *Elsevier Ltd*. doi: 10.1016/j.jallcom.2018.01.298.

- [39] R. Chu *et al.*, “Long-term cycling of core-shell Fe<sub>3</sub>O<sub>4</sub>-Polypyrrole composite electrodes via diffusive and capacitive lithiation,” *J Alloys Compd*, vol. 835, Sep. 2020, doi: 10.1016/j.jallcom.2020.155192.
- [40] J. Zhang, K. Wang, Q. Xu, Y. Zhou, F. Cheng, and S. Guo, “Beyond yolk-shell nanoparticles: Fe<sub>3</sub>O<sub>4</sub>@Fe<sub>3</sub>C Core@Shell nanoparticles as yolks and carbon nanospindles as shells for efficient lithium ion storage,” *ACS Nano*, vol. 9, no. 3, pp. 3369–3376, Mar. 2015, doi: 10.1021/acsnano.5b00760.
- [41] M. V. Reddy *et al.*, “ $\alpha$ -Fe<sub>2</sub>O<sub>3</sub> nanoflakes as an anode material for li-ion batteries,” *Adv Funct Mater*, vol. 17, no. 15, pp. 2792–2799, Oct. 2007, doi: 10.1002/adfm.200601186.
- [42] J. Li *et al.*, “Phase evolution of conversion-type electrode for lithium ion batteries,” *Nat Commun*, vol. 10, no. 1, Dec. 2019, doi: 10.1038/s41467-019-09931-2.
- [43] M. A. Rahman, R. Radhakrishnan, and R. Gopalakrishnan, “Structural, optical, magnetic and antibacterial properties of Nd doped NiO nanoparticles prepared by co-precipitation method,” Apr. 25, 2018, *Elsevier Ltd.* doi: 10.1016/j.jallcom.2018.01.298.
- [44] Y. Chen, B. Song, M. Li, L. Lu, and J. Xue, “Fe<sub>3</sub>O<sub>4</sub> Nanoparticles embedded in uniform mesoporous carbon spheres for superior High-rate battery applications,” *Adv Funct Mater*, vol. 24, no. 3, pp. 319–326, Jan. 2014, doi: 10.1002/adfm.201300872.
- [45] J. Li *et al.*, “Phase evolution of conversion-type electrode for lithium ion batteries,” *Nat Commun*, vol. 10, no. 1, Dec. 2019, doi: 10.1038/s41467-019-09931-2.
- [46] B. Wang, J. S. Chen, H. Bin Wu, Z. Wang, and X. W. Lou, “Quasiemulsion-templated formation of  $\alpha$ -Fe<sub>2</sub>O<sub>3</sub> hollow spheres with enhanced lithium storage properties,” *J Am Chem Soc*, vol. 133, no. 43, pp. 17146–17148, Nov. 2011, doi: 10.1021/ja208346s.
- [47] J. Li *et al.*, “Phase evolution of conversion-type electrode for lithium ion batteries,” *Nat Commun*, vol. 10, no. 1, Dec. 2019, doi: 10.1038/s41467-019-09931-2.
- [48] R. Chu *et al.*, “Long-term cycling of core-shell Fe<sub>3</sub>O<sub>4</sub>-Polypyrrole composite electrodes via diffusive and capacitive lithiation,” *J Alloys Compd*, vol. 835, Sep. 2020, doi: 10.1016/j.jallcom.2020.155192.
- [49] Sungjemmenla, S. K. Vineeth, C. B. Soni, V. Kumar, and Z. W. Seh, “Understanding the Cathode–Electrolyte Interphase in Lithium-Ion Batteries,” Sep. 01, 2022, *John Wiley and Sons Inc.* doi: 10.1002/ente.202200421.
- [50] J. Luo *et al.*, “Three-dimensional graphene foam supported Fe<sub>3</sub>O<sub>4</sub> lithium battery anodes with long cycle life and high rate capability,” *Nano Lett*, vol. 13, no. 12, pp. 6136–6143, Dec. 2013, doi: 10.1021/nl403461n.
- [51] L. Wang, Y. Yu, P. C. Chen, D. W. Zhang, and C. H. Chen, “Electrospinning synthesis of C/Fe<sub>3</sub>O<sub>4</sub> composite nanofibers and their application for high

- performance lithium-ion batteries,” *J Power Sources*, vol. 183, no. 2, pp. 717–723, Sep. 2008, doi: 10.1016/j.jpowsour.2008.05.079.
- [52] U. Boesenberg *et al.*, “Asymmetric pathways in the electrochemical conversion reaction of NiO as battery electrode with high storage capacity,” *Sci Rep*, vol. 4, 2014, doi: 10.1038/srep07133.
- [53] A. Kumar Rai, L. Tuan Anh, C. J. Park, and J. Kim, “Electrochemical study of NiO nanoparticles electrode for application in rechargeable lithium-ion batteries,” *Ceram Int*, vol. 39, no. 6, pp. 6611–6618, Aug. 2013, doi: 10.1016/j.ceramint.2013.01.097.
- [54] G. Zhou *et al.*, “Progress of NiO-Based Anodes for High-Performance Li-Ion Batteries,” Oct. 01, 2022, *John Wiley and Sons Inc.* doi: 10.1002/tcr.202200111.
- [55] W. Lv *et al.*, “A sandwich structure of graphene and nickel oxide with excellent supercapacitive performance,” *J Mater Chem*, vol. 21, no. 25, pp. 9014–9019, Jul. 2011, doi: 10.1039/c1jm10400d.
- [56] L. Yu *et al.*, “Fabrication of carbon-coated NiO supported on graphene for high performance supercapacitors,” *RSC Adv*, vol. 6, no. 17, pp. 14199–14204, 2016, doi: 10.1039/c6ra01405d.
- [57] Y. Yu, Y. Liu, and X. Yang, “Carbon Nanofiber-Based Materials as Anode Materials for Lithium-Ion Batteries,” in *Alkali-ion Batteries*, InTech, 2016. doi: 10.5772/63235.
- [58] Z. Wang, M. Zhang, and J. Zhou, “Flexible NiO-Graphene-Carbon Fiber Mats Containing Multifunctional Graphene for High Stability and High Specific Capacity Lithium-Ion Storage,” *ACS Appl Mater Interfaces*, vol. 8, no. 18, pp. 11507–11515, May 2016, doi: 10.1021/acsami.6b01958.
- [59] D. Xie, Q. Su, W. Yuan, Z. Dong, J. Zhang, and G. Du, “Synthesis of porous NiO-wrapped graphene nanosheets and their improved lithium storage properties,” *Journal of Physical Chemistry C*, vol. 117, no. 46, pp. 24121–24128, Nov. 2013, doi: 10.1021/jp4054814.
- [60] M. Serhan *et al.*, “Total iron measurement in human serum with a smartphone,” in *AICHE Annual Meeting, Conference Proceedings*, American Institute of Chemical Engineers, 2019. doi: 10.1039/x0xx00000x.
- [61] Ata-ur-Rehman *et al.*, “Current advances and prospects in NiO-based lithium-ion battery anodes,” Oct. 01, 2022, *Elsevier Ltd.* doi: 10.1016/j.seta.2022.102376.
- [62] K. Zhang *et al.*, “Nitrogen-doped porous interconnected double-shelled hollow carbon spheres with high capacity for lithium-ion batteries and sodium ion batteries,” *Electrochim Acta*, vol. 155, pp. 174–182, Feb. 2015, doi: 10.1016/j.electacta.2014.12.108.
- [63] J. Zang *et al.*, “Hollow-in-hollow carbon spheres with hollow foam-like cores for lithium–sulfur batteries,” *Nano Res*, vol. 8, no. 8, pp. 2663–2675, Aug. 2015, doi: 10.1007/s12274-015-0773-3.



- [64] X. Zhang, X. Liu, J. Zhou, C. Qin, and Z. Wang, “Improving the cycling stability of Fe<sub>3</sub>O<sub>4</sub>/NiO anode for lithium ion battery by constructing novel bimodal nanoporous urchin network,” *Nanomaterials*, vol. 10, no. 9, pp. 1–9, Sep. 2020, doi: 10.3390/nano10091890.
- [65] C. Zhang, Q. Zhou, H. Wang, J. Liu, Y. Zhang, and S. Wang, “The effects of binders on the lithium storage of Fe<sub>3</sub>O<sub>4</sub>/NiO heterostructures,” *Ionics (Kiel)*, vol. 29, no. 9, pp. 3573–3584, Sep. 2023, doi: 10.1007/s11581-023-05074-z.
- [66] Q. Wu *et al.*, “Hydrogenated titanium dioxide modified core–shell structure Fe<sub>3</sub>O<sub>4</sub>@NiO for lithium-ion battery anode material,” *Ionics (Kiel)*, vol. 29, no. 6, pp. 2227–2240, Jun. 2023, doi: 10.1007/s11581-023-04990-4.
- [67] Y. Chen, B. Song, M. Li, L. Lu, and J. Xue, “Fe<sub>3</sub>O<sub>4</sub> Nanoparticles embedded in uniform mesoporous carbon spheres for superior High-rate battery applications,” *Adv Funct Mater*, vol. 24, no. 3, pp. 319–326, Jan. 2014, doi: 10.1002/adfm.201300872.
- [68] G. Zhou *et al.*, “Progress of NiO-Based Anodes for High-Performance Li-Ion Batteries,” Oct. 01, 2022, *John Wiley and Sons Inc.* doi: 10.1002/tcr.202200111.
- [69] Ata-ur-Rehman *et al.*, “Current advances and prospects in NiO-based lithium-ion battery anodes,” Oct. 01, 2022, *Elsevier Ltd.* doi: 10.1016/j.seta.2022.102376.
- [70] K. Zhang *et al.*, “Nitrogen-doped porous interconnected double-shelled hollow carbon spheres with high capacity for lithium ion batteries and sodium ion batteries,” *Electrochim Acta*, vol. 155, pp. 174–182, Feb. 2015, doi: 10.1016/j.electacta.2014.12.108.
- [71] X. Zhang, X. Liu, J. Zhou, C. Qin, and Z. Wang, “Improving the cycling stability of Fe<sub>3</sub>O<sub>4</sub>/NiO anode for lithium ion battery by constructing novel bimodal nanoporous urchin network,” *Nanomaterials*, vol. 10, no. 9, pp. 1–9, Sep. 2020, doi: 10.3390/nano10091890.
- [72] M. A. Rahman, R. Radhakrishnan, and R. Gopalakrishnan, “Structural, optical, magnetic and antibacterial properties of Nd doped NiO nanoparticles prepared by co-precipitation method,” Apr. 25, 2018, *Elsevier Ltd.* doi: 10.1016/j.jallcom.2018.01.298.
- [73] M. A. Rahman, R. Radhakrishnan, and R. Gopalakrishnan, “Structural, optical, magnetic and antibacterial properties of Nd doped NiO nanoparticles prepared by co-precipitation method,” Apr. 25, 2018, *Elsevier Ltd.* doi: 10.1016/j.jallcom.2018.01.298.
- [74] F. Su, X. S. Zhao, Y. Wang, L. Wang, and J. Y. Lee, “Hollow carbon spheres with a controllable shell structure,” *J Mater Chem*, vol. 16, no. 45, pp. 4413–4419, 2006, doi: 10.1039/b609971h.
- [75] M. A. Rahman, R. Radhakrishnan, and R. Gopalakrishnan, “Structural, optical, magnetic and antibacterial properties of Nd doped NiO nanoparticles prepared by

- co-precipitation method,” Apr. 25, 2018, *Elsevier Ltd.* doi: 10.1016/j.jallcom.2018.01.298.
- [76] A. Stegarescu *et al.*, “Synthesis and Characterization of MWCNT-COOH/Fe<sub>3</sub>O<sub>4</sub> and CNT-COOH/Fe<sub>3</sub>O<sub>4</sub>/NiO Nanocomposites: Assessment of Adsorption and Photocatalytic Performance,” *Nanomaterials*, vol. 12, no. 17, Sep. 2022, doi: 10.3390/nano12173008.
- [77] Z. Xue, L. Li, L. Cao, W. Zheng, W. Yang, and X. Yu, “A simple method to fabricate NiFe<sub>2</sub>O<sub>4</sub>/NiO@Fe<sub>2</sub>O<sub>3</sub> core-shelled nanocubes based on Prussian blue analogues for lithium ion battery,” *J Alloys Compd*, vol. 825, Jun. 2020, doi: 10.1016/j.jallcom.2020.153966.
- [78] X. Ma, W. Zhao, K. Lu, C. Zhang, C. Yuan, and K. L. Tang, “Spindle-like Fe<sub>3</sub>O<sub>4</sub>/NiO/N-Doped Carbon Nanocomposites for High-Performance Nitrite and Hydrogen Peroxide Sensing,” *ACS Appl Nano Mater*, vol. 7, no. 9, pp. 9978–9990, May 2024, doi: 10.1021/acsanm.4c00200.
- [79] K. K. Kara and G. Rabbani, “Experimental Study of Methylene Blue Adsorption from Aqueous Solutions onto Fe<sub>3</sub>O<sub>4</sub>/NiO Nano Mixed Oxides Prepared by Ultrasonic Assisted Co-precipitation,” *J Nanostruct*, vol. 9, no. 2, pp. 287–300, 2019, doi: 10.22052/JNS.2019.02.011.
- [80] A. Stegarescu *et al.*, “Synthesis and Characterization of MWCNT-COOH/Fe<sub>3</sub>O<sub>4</sub> and CNT-COOH/Fe<sub>3</sub>O<sub>4</sub>/NiO Nanocomposites: Assessment of Adsorption and Photocatalytic Performance,” *Nanomaterials*, vol. 12, no. 17, Sep. 2022, doi: 10.3390/nano12173008.
- [81] Z. Xue, L. Li, L. Cao, W. Zheng, W. Yang, and X. Yu, “A simple method to fabricate NiFe<sub>2</sub>O<sub>4</sub>/NiO@Fe<sub>2</sub>O<sub>3</sub> core-shelled nanocubes based on Prussian blue analogues for lithium ion battery,” *J Alloys Compd*, vol. 825, Jun. 2020, doi: 10.1016/j.jallcom.2020.153966.
- [82] C. Zhang, Q. Zhou, H. Wang, J. Liu, Y. Zhang, and S. Wang, “The effects of binders on the lithium storage of Fe<sub>3</sub>O<sub>4</sub>/NiO heterostructures,” *Ionics (Kiel)*, vol. 29, no. 9, pp. 3573–3584, Sep. 2023, doi: 10.1007/s11581-023-05074-z.
- [83] X. Zhang, X. Liu, J. Zhou, C. Qin, and Z. Wang, “Improving the cycling stability of Fe<sub>3</sub>O<sub>4</sub>/NiO anode for lithium ion battery by constructing novel bimodal nanoporous urchin network,” *Nanomaterials*, vol. 10, no. 9, pp. 1–9, Sep. 2020, doi: 10.3390/nano10091890.
- [84] Q. Wu *et al.*, “Hydrogenated titanium dioxide modified core-shell structure Fe<sub>3</sub>O<sub>4</sub>@NiO for lithium-ion battery anode material,” *Ionics (Kiel)*, vol. 29, no. 6, pp. 2227–2240, Jun. 2023, doi: 10.1007/s11581-023-04990-4.